NTIA Report 91-275

A Model of Millimeter-Wave Propagation for Personal Communication Networks in Urban Settings

Kenneth C. Allen

U.S. DEPARTMENT OF COMMERCE
Robert A. Mosbacher, Secretary

Janice Obuchowski, Assistant Secretary
for Communications and Information

April 1991

Product Disclaimer

Certain commercial equipment, instruments, or materials are identified in this paper to specify adequately the technical aspects of the reported results. In no case does such identification imply recommendation or endorsement by the National Telecommunications and Information Administration, nor does it imply that the material or equipment identified is necessarily the best available for the purpose.

CONTENTS

LIST OF FIGURES

A MODEL OF MILLIMETER-WAVE PROPAGATION FOR PERSONAL COMMUNICATION NETWORKS IN URBAN SETTINGS

K.C. Allen*

Rapid development of personal, portable, radio communications is expected during this decade. A primary example of this is the emergence of personal communication networks (PCN). These networks are similar to today's cellular telephone technology. However, much smaller cell sizes are used and, as a result, the portable phone is much smaller (pocket size) and inexpensive. The use of millimeter waves for PCN services offers many advantages. Models of millimeter-wave propagation on the kinds of paths that will occur in small cells are needed. In this report a geometrical optics model of the propagation of millimeter waves for line-of-sight paths near street level in urban environments is developed. An idealized environment is assumed with flat streets and uniform street widths between flat building walls. The image-space approach is used to index the direct line-of-sight ray and all reflected ray paths between the transmitter and receiver. The model can be used to simulate received signal characteristics for testing system designs. The statistical behavior of signal level can be computed from the model for real world environments for which it is not practical to give a complete description of the complex physical geometry. The model also shows the channel impulse response functions to be expected in urban cells. Calculations from the model are compared with data measured in downtown Denver at 9.6, 28.8, and 57.6 GHz.

Key words: impulse response; millimeter waves; PCN; personal communication networks; propagation; urban

1. INTRODUCTION

In order to take advantage of millimeter waves for personal communication networks (PCN), their propagation on short paths in various environments needs to be adequately modeled. A model is developed here of millimeter-wave propagation in an outdoor urban environment for line-of-sight paths of the type that would be expected in a PCN cell.

The propagation of millimeter waves (30-300 GHz) in an urban environment is complex because of the numerous opportunities for attenuation, reflection, scattering, and diffraction. A general, full-wave solution or model is unrealistic because of the physical

* The author is with the Institute for Telecommunication Sciences, National Telecommunications and Information Administration, U.S. Department of Commerce, Boulder, Colorado 80303.

complexity of the environment. However, a practical model using geometrical optics theory has been developed for line-of-sight paths. Although it does not give an exact solution for a given unique urban environment, it does give predictions that are qualitatively and statistically similar to measured results.

The model is valuable for the information it gives about which modes of propagation are most important in the urban setting. It also can be used to predict a priori statistics of signal level and other parameters based on simple descriptions of the urban environment (e.g., street width) and the radio equipment.

The comparison between the predictions of the geometrical optics or ray model and measured data was very fruitful. Some of the similarities aided in the interpretation of features in the measured data while the differences revealed some of the limitations of the model.

In section 2, background material is presented that illuminates the purpose of the model and the reason for approaching the problem from the geometrical optics point of view. In section 3, a description of the model is presented. In section 4, outputs from software developed to implement the model are explained. These outputs provide examples of the types of predictions possible from the model. In section 5, comparisons are made between the model predictions and measured data. A summary is given in section 6 and the ray geometry software is given in the appendix.

2. BACKGROUND

It is widely expected that land mobile radio systems will evolve towards personal communications networks (PCN) during this decade. PCN will allow people to connect into the telephone system with small (pocket size) portable phones. Ultimately, portable, wideband, digital service may be available to users.

These PCN services will be based on cellular technology where the cell sizes are expected to be smaller than today's cellular telephone cells. The primary advantage of small cells is that they allow the user's terminal to be small, low powered, and inexpensive. Outdoor cells the size of neighborhoods, stadiums, and a few blocks in downtown urban areas are anticipated. Indoor cells may range in size from shopping malls and factories to individual rooms.

Radio frequency bands around 900 and 1800 MHz are already being considered. In addition, millimeter waves are of interest, especially for the anticipated wideband, digital services of the future. The critical market issue is: will the growth of the service be limited by the cost to the user or by a shortage of bandwidth?

2.1 Advantages of Millimeter Waves for PCN

The millimeter-wave band (30-300 GHz) offers many advantages for personal, mobile, radio communications. These advantages include: spectrum availability, small size of components, integrated circuit manufacturing technology, and frequency reuse in cells a short distance away because of atmospheric absorption.

2.1.1 Spectrum availability

One of the growing telecommunication issues of this decade is spectrum availability. A myriad of new radio services including, but not limited to, wireless local area networks, high-definition television, mobile satellite communications, cellular telephone, direct satellite broadcast of sound and television, and PCN all require radio spectrum. Finding spectrum for these new services is difficult.

Spectrum in the higher portions of the radio band has not been utilized because of the high cost of the hardware and because the propagation of these higher frequency radio waves is not as well understood as in the lower bands. As a result, the millimeter-wave band remains essentially empty.

It would be much easier to find spectrum for PCN services in the millimeter-wave band than at lower frequencies, especially for the bandwidth required to provide wideband, digital services.

2.1.2 Millimeter-wave hardware advantages

The technology to produce millimeter-wave devices has been progressing rapidly. The cost of some systems have decreased to one-third of what they were a decade ago. Two developing technologies, in particular, hold promise of providing inexpensive millimeter-wave devices. One is the monolithic millimeter-wave integrated circuit (MMIC). The other is the high electron mobility transistor (HEMT). HEMT technology promises inexpensive, high-quality amplifiers for frequencies up to 100 GHz, which can easily be incorporated into MMIC products.

For millimeter waves, radio frequency devices can be quite small, so that in fact, complete digital radio transceivers can be produced on a single integrated circuit chip. This gives the two advantages of low manufacturing cost and small size for the portable phone. Certainly, if millimeter waves were used for PCN services, the cost of millimeter-wave devices would decrease even more because of the economy of scale.

2.1.3 Millimeter-wave propagation advantages

Millimeter waves are absorbed by oxygen and water vapor in the atmosphere. The absorption rate by water vapor depends on how much water vapor is present. For frequencies below about 70 GHz, the absorption rate by water vapor is less than 1 dB/km. However, absorption by oxygen is about 15 dB/km in a band centered around 60 GHz. The absorption of millimeter waves by the atmosphere is accurately known (Liebe, 1985). The atmospheric absorption rate at sea level for several values of relative humidity is shown in Figure 1.

Absorption of millimeter waves near 60 GHz by the atmosphere is a very desirable effect for cellular radio applications. With proper cell design, the absorption will have a relatively minor effect within the cell. At distances larger than the radius of the designed cell, the signal will be rapidly attenuated. Moreover, this attenuation is certain and cannot be overcome by anomalous propagation effects. This greatly reduces the size of the region about a cell where the signal is unreliable for communications but is still so strong on occasion that re-use of the frequency in another cell is prohibited by the potential for interference. Atmospheric absorption can therefore actually increase the capacity of services that can be provided within a given bandwidth.

Another advantage of millimeter waves is that the short wave length results in much smaller antenna requirements. In fact, a small portable phone may be large enough to contain several antennas that can be used to provide spatial diversity improvement. The short wavelengths mean that only a small antenna spacing is required to get diversity improvement.

2.2 Millimeter-Wave Propagation Measurements for PCN

If millimeter waves are to be used for PCN services, the propagation of millimeter waves in outdoor and indoor cells needs to be understood. Measurements have been made

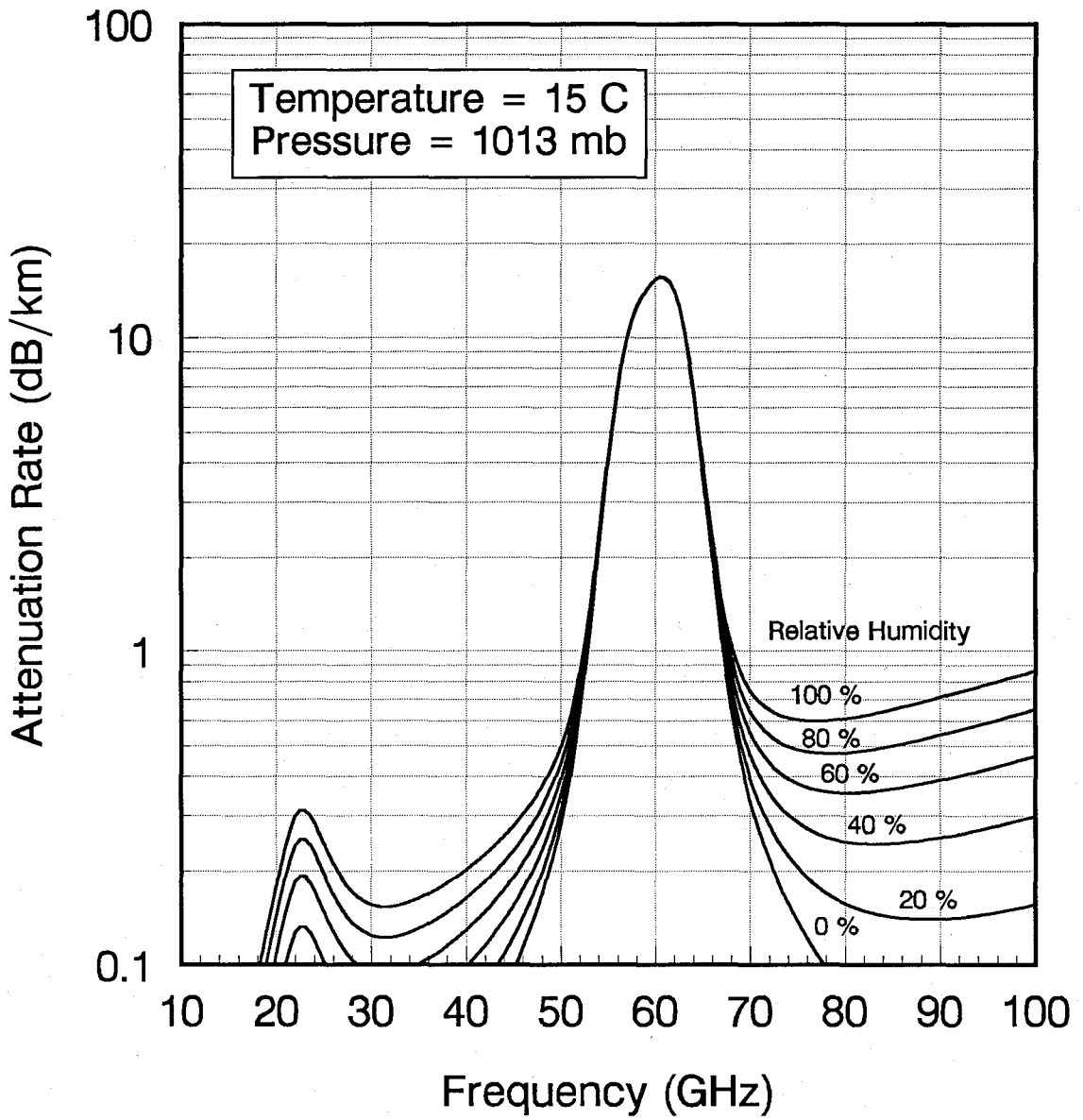

Figure 1. The absorption of millimeter-waves at sea level by the atmosphere for several values of relative humidity.

on the kinds of paths expected in PCN service cells (Violette et al., 1983, 1985, 1988a and 1988b). These measurements include propagation in urban and suburban settings. Measurements of diffraction around and over obstacles, and of wideband impulse response in downtown urban areas are reported.

The author found that the geometrical theory of diffraction adequately described the above diffraction measurements. It was also found that a model based on geometrical optics theory adequately described line-of-sight propagation measurements from urban areas. It is the geometrical optics model and its comparison to the measurements that are the primary subject of this report.

The measurements were made in downtown Denver, Colorado. A photograph of one of the streets on which measurements were made is shown in Figure 2. The measurements were made at night when the streets were nearly devoid of traffic.

Among the different measurements made were azimuth angle scans where the transmitting antenna would be moved in azimuth angle while the receiving antenna was fixed and the signal amplitude was recorded. Upon examination of the data, i.e., signal amplitude as a function of azimuth angle, it was determined that most of the radio frequency energy arriving at the receiver was either line-of-sight or reflected from the building walls that lined the streets. Peak received signal levels were found at azimuth angles that corresponded to the angles of arrival that would be expected for ray paths having 1, 2, 3, and even 4 reflections from the building walls. Very little energy appeared to have been scattered or diffracted into the receiving antenna.

It therefore seemed reasonable that a model based on geometrical optics or ray paths would adequately describe millimeter-wave propagation in such urban environments. It was desired that the model display the same qualitative characteristics and have the same statistics as the observed data. Comparison of the model predictions to observed data would then serve two purposes. First, it would help identify the propagation effects that caused features observed in the data, increasing the understanding of the measured data. Secondly, it would show how the model can be improved to better account for the propagation effects actually observed, i.e., the limits of the model would be better understood.

After validation of the model is accomplished, it can be used to predict the propagation effects of different scenarios. This is of course the real value of the model, the

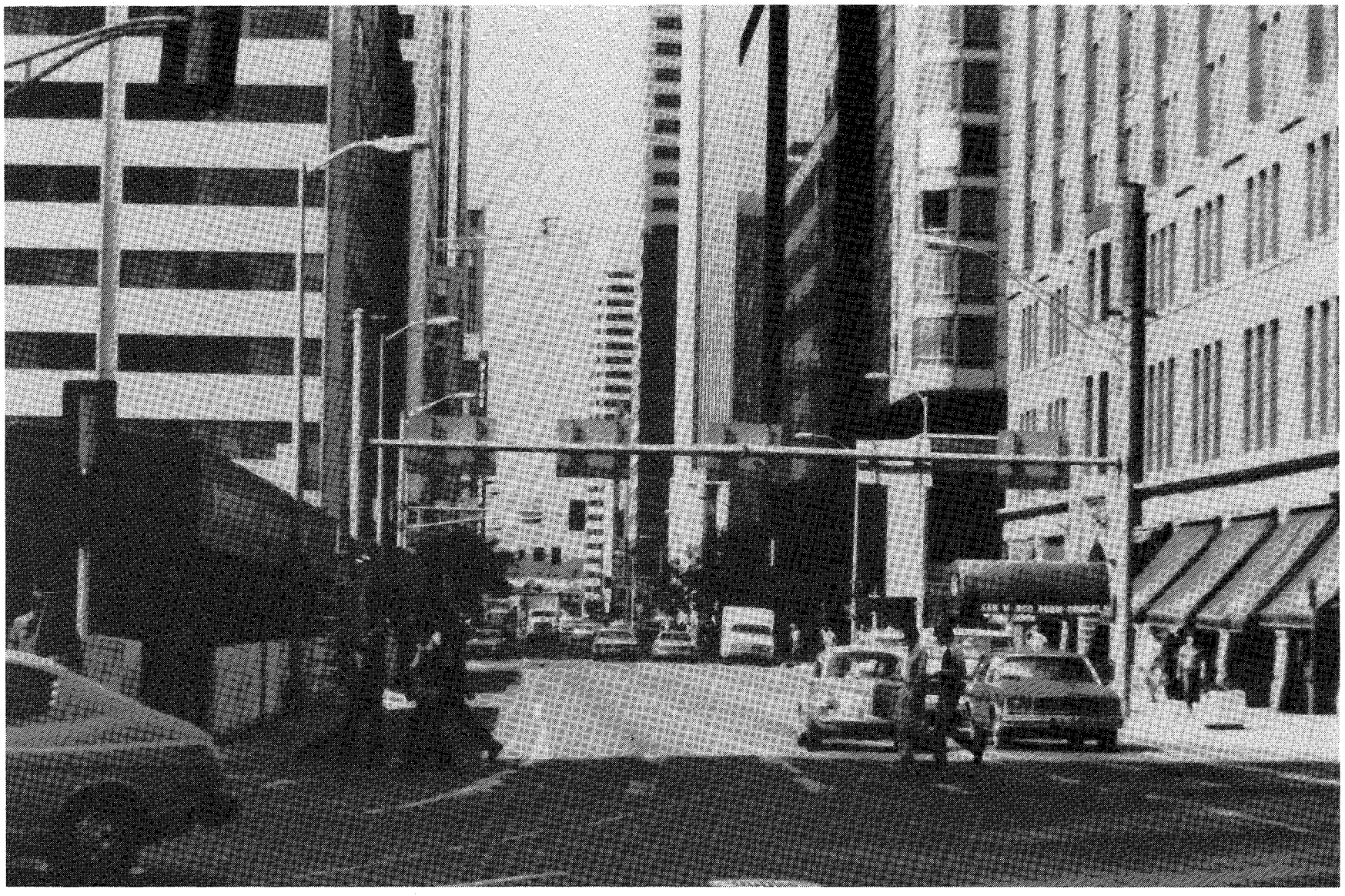

Figure 2. The intersection of Broadway and 17th Street (looking west) where many of the measurements were made.

ability to predict results without having to measure them. The performance of telecommunication equipment can then be evaluated or predicted using the model before the equipment is built and tested.

An advantage of a geometrical optics or ray model is that although it is not a full-wave model it does give a complete description of the propagation. The impulse response, signal amplitude, and signal phase can all be found as a function of frequency, antenna position, antenna pointing, antenna beamwidth, etc.

3. DESCRIPTION OF THE MODEL

3.1 Idealized Physical Model

In order to make the model mathematically tractable and no more complex than necessary, an idealized physical model of the urban environment is used. The street is assumed to be perfectly flat. The building walls are also assumed to be perfectly flat and the width of the street, i.e., the distance between the building walls, is constant. Figure 3 depicts the idealized environment. After the model was complete, it was found that because of the mathematical treatment given the rays, the predictions agreed better with the observed data if no cross streets were used. Thus, we end up with a waveguide that is open on one side.

This idealized physical model simplifies a complex environment but preserves the basic elements that have the greatest effect on propagation. The shallow reflection angles involved in the geometry make this possible. Although irregularities in the physical composition and distance of the building fronts from the center of the street will effect the amplitude and phase of reflected signals at the receiver, the geometry or angles to the receiver and transmitter are not effected significantly. The effects of variations in building distance from the street center, cross streets, and scattering from objects are discussed later.

3.2 The Mathematical Model

To develop the mathematical model, geometrical optics or ray theory is used. The received signal is assumed to consist of the sum of a number of rays. These rays arrive at the antenna either directly from the transmitter or after reflection from the street and walls.

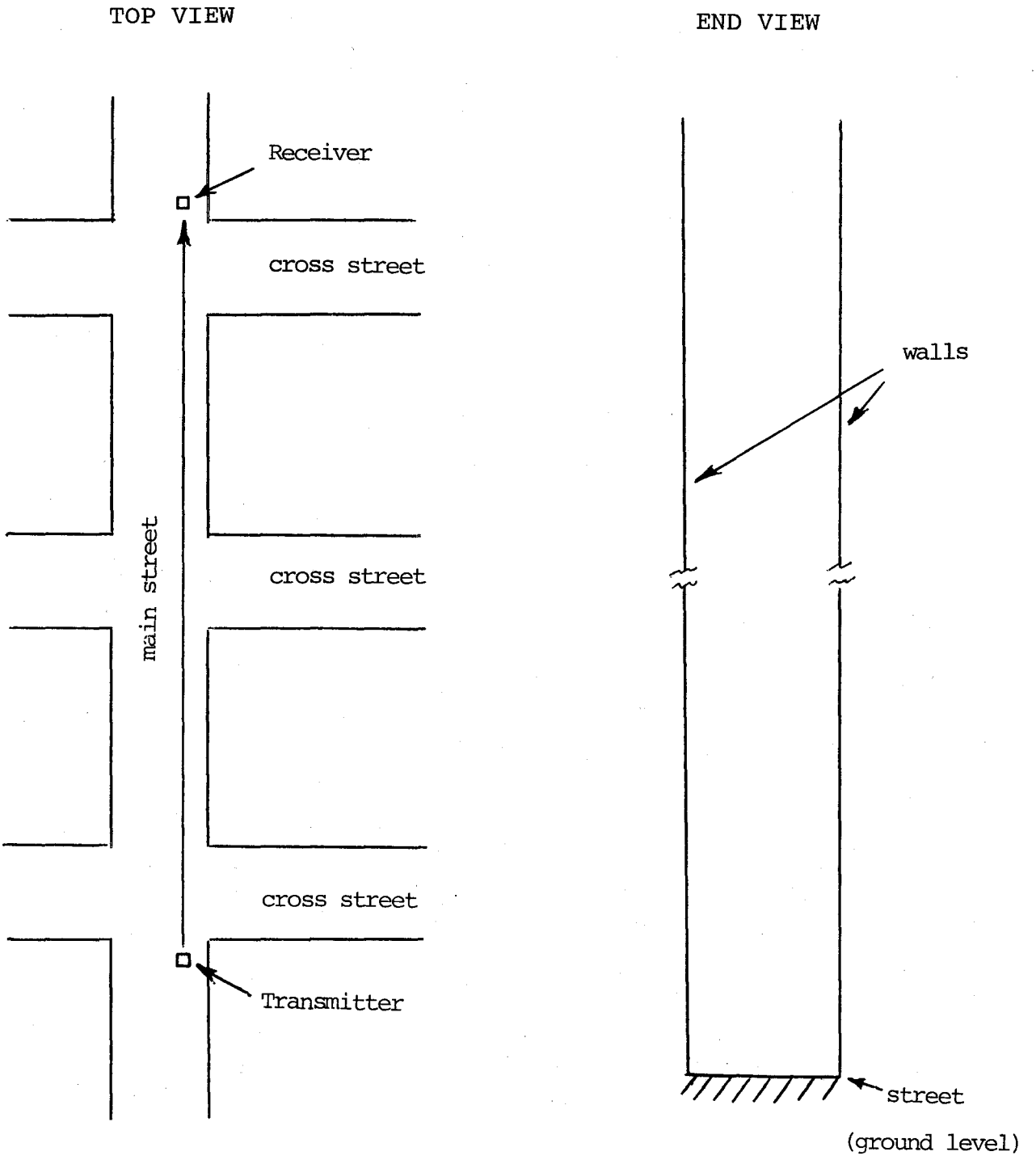

Figure 3. Top and end (side) views of idealized street environment.

Specular reflection is assumed with separate, but constant, values for the coefficients of reflection for the walls and street.

The idealized physical model makes for simple accounting of all the possible rays from the transmitter to the receiver. The reflections from the street and walls are dealt with by using the image space. Multiple images of the receiver rather than of the transmitter are used here. That is, a ray reflected from a wall appears to be arriving at an image of the receiver beyond the wall.

3.2.1 Ray geometry

In Figure 4a, the coordinate system convention used is shown. In Figures 4b and 4c, the locations of the receiver images are shown along with the ray paths. Each receiver image in Figure 4b corresponds to one ray path to the real receiver. Each image is given a double index. The first index, N, gives the number of wall reflections. A negative or positive sign corresponds to the first reflection being to the left or right of the transmitter, respectively, when looking towards the receiver. Thus, all the images for which this index is negative are to the left of the transmitter and all the positive ones are to the right. The second index, M, indicates whether or not the ray has reflected from the street. A value of positive one means the ray is not reflected from the street and the image is above ground level. A value of negative one indicates the ray is reflected from the street and the image is below ground level. The index (0,1) corresponds to the real receiver location and the direct line-of-sight ray.

The geometry of each ray is easily computed from the location of each receiver image and the sum of the rays is found by looping through the double index of the images. The location of the transmitter is (X_t,Y_t,Z_t) as shown in Figure 4. The location of the receiver shown in the same figure is (X_r,Y_r,Z_r) and the street width is W. For convenience, it will be assumed that $Y_t=0$ so that the receiver is a distance Y_r down the street from the transmitter. The location of each receiver image is given by the coordinates

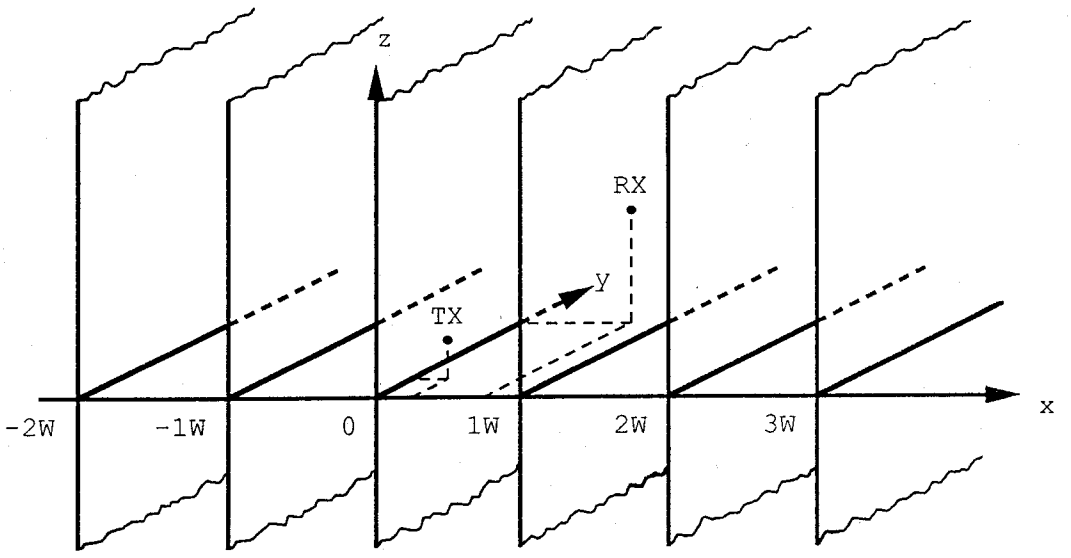

a. Image streets created to each side.

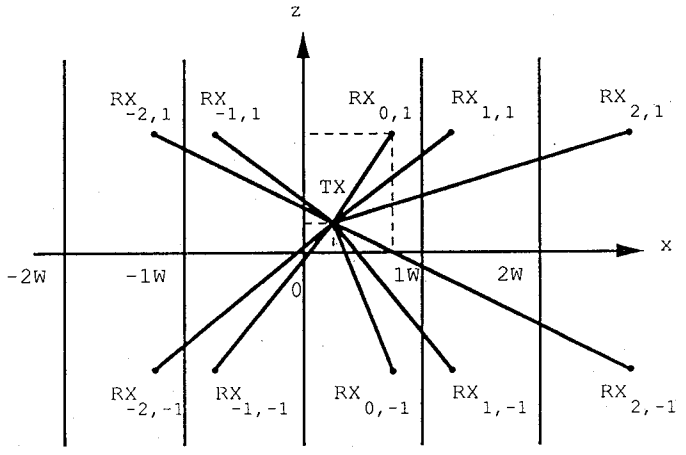

b. Imaging for street and wall reflected rays as seen looking down street (end view).

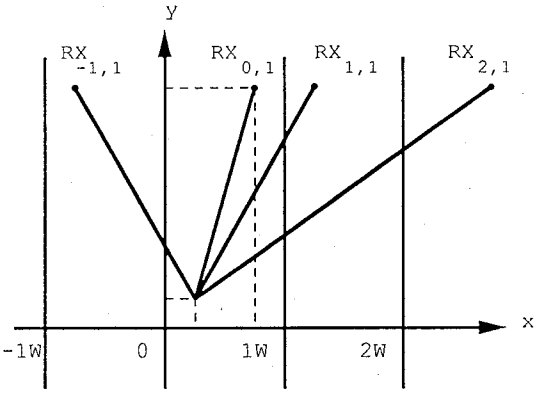

c. Above ground wall reflection rays in image space as seen from above.

Figure 4. Diagrams of the image space description of ray paths.

$$X_{N,M} = (N+(1-(-1)^N)/2)W+(-1)^N X_r, \tag{1}$$

$$Y_{N,M} = Y_r, \tag{2}$$

$$Z_{N,M} = MZ_r, \tag{3}$$

where N and M are the first and second indices of the image, respectively, as defined above.

The length of each ray is given by

$$L = \sqrt{(X-X_t)^2+Y^2+(Z-Z_t)^2}, \tag{4}$$

where the indices have been dropped from the coordinates of the receiver image location. The horizontal length of each ray, i.e., the length of the ray projected onto the x-y plane is

$$L_h = \sqrt{(X-X_t)^2+Y^2}. \tag{5}$$

The azimuthal angle (in the x-y plane) of the ray from the transmitter to the receiver is

$$\alpha_t = \arctan((X-X_t)/Y), \tag{6}$$

where a negative angle is to the left and a positive one is to the right when standing at the transmitter facing the receiver. The azimuthal angle from the receiver to the transmitter is

$$\alpha_r = \alpha_t(-1)^N, \tag{7}$$

where the N dependence accounts for the change in direction caused by each reflection from the walls. Again, when looking towards the other terminal, a negative angle is to the left and a positive one is to the right.

The elevation angle from the transmitter to the receiver is

$$\beta_t = \arctan((Z-Z_t)/L_h), \tag{8}$$

and the elevation angle from the receiver to the transmitter is

$$\beta_r = -M\beta_t. \tag{9}$$

The elevation angles are measured with respect to the horizontal with a positive angle being above horizontal and a negative one, below horizontal.

The formula for the true angle between two intersecting lines in three dimensional space,

$$T = \arccos\left[\frac{A_1A_2+B_1B_2+C_1C_2}{\sqrt{A_1^2+B_1^2+C_1^2}\sqrt{A_2^2+B_2^2+C_2^2}}\right], \tag{10}$$

is very useful here. The variables A_1, B_1, and C_1 are the direction ratios of the first line and A_2, B_2, and C_2 are the direction ratios of the second line. The direction ratios can be thought of as the change in each of the linear geometric coordinates when moving from one end to the other of an arbitrarily fixed length of the line. The set of direction ratios for each line can be multiplied by arbitrary constants with no effect on the true angle given by (10). This formula is easily derived from the dot product of two line segments.

Using (10), the angle of reflection from the street with respect to the normal to the street is found to be

$$\alpha_s = \arccos((Z-Z_t)/L). \tag{11}$$

The angles of reflection from the walls with respect to the normal to the walls are all equal, as can be seen in Figure 4, and again are found from (10) to be

$$\alpha_w = \arccos((X-X_t)/L). \tag{12}$$

A ray to the receiver image with first index N has a total number of reflections from the walls equal to the absolute value of N. These reflections alternate between the left and

right walls so that the x-coordinate, X_w, equals 0 or W. If $N>0$, the images are to the right so that the first reflection is from the right wall. The x-coordinate of the I^{th} reflection is then given by

$$X_w = ((1-(-1)^I)/2)W, \qquad \text{for } N>0. \tag{13}$$

The other coordinates are given by

$$Y_w = Y_t + (IW-X_t)(Y-Y_t)/(X-X_t), \qquad \text{for } N>0, \tag{14}$$

and

$$Z_w = |Z_t + (IW-X_t)(Z-Z_t)/(X-X_t)|, \qquad \text{for } N>0. \tag{15}$$

When $N<0$, the images are to the left and the first reflection is from the left wall. The x-coordinate of the I^{th} reflection is then given by

$$X_w = ((1+(-1)^I)/2)W, \qquad \text{for } N<0. \tag{16}$$

The other coordinates are given by

$$Y_w = Y_t + ((1-I)W-X_t)(Y-Y_t)/(X-X_t), \qquad \text{for } N<0, \tag{17}$$

and

$$Z_w = |Z_t + ((1-I)W-X_t)(Z-Z_t)/(X-X_t)|, \qquad \text{for } N<0. \tag{18}$$

For the street (ground) reflection (M=-1), the z-coordinate is of course zero, Z_s=0. The y-coordinate is given by

$$Y_s = Y_t - Z_t(Y-Y_t)/(Z-Z_t). \tag{19}$$

The derivation of the real x-coordinate of the ground reflection is somewhat more complex because of the folding in the image space along the x-axis. In the image space, the x-coordinate of the ground reflection is given by

$$\hat{X}_s = X_t - Z_t(X-X_t)/(Z-Z_t). \tag{20}$$

Another useful variable is given by

$$I_s = [\hat{X}_s/W] - u(-N), \tag{21}$$

where u(•) denotes the unit-step function, i.e., u(x)=0 if x<=0 and u(x)=1 if x>0, and [•] denotes the integer function. The variable, I_s, is the index of the image of the street in which the ground reflection occurs and is zero for the real street. If I_s is odd, the street image is reversed, i.e., a mirror image. If I_s is even, the image has the same left and right orientation as the real street (see Figure 4c). The x-coordinate location of the ground reflection in the real street is given by

$$X_s = \hat{X}_s - I_s W, \qquad \text{for even } I_s, \tag{22}$$

and

$$X_s = W - (\hat{X}_s - I_s W), \qquad \text{for odd } I_s. \tag{23}$$

3.2.2 Ray amplitude

In the model developed here for the idealized environment, the ray amplitude is determined by a number of factors; the transmitter power, P_t, the transmitter and receiver antenna gains, G_t and G_r, the losses due to reflection from the walls and street, L_r, the absorption due to water vapor and dry air, L_a, and of course, the free-space loss, L_f. The ray amplitude, A, at the receiver is therefore given by

$$A = P_t + G_t + G_r - L_f - L_r - L_a, \tag{24}$$

where all the quantities are in dB (A and P_t in dBm).

The free-space loss is

$$L_f = 20\log(4\pi L/\lambda) = 32.45 + 20\log(FL), \tag{25}$$

where λ is the wavelength, L is distance, both in meters, and the radio frequency, F, is in GHz.

Assuming parabolic dish antennas, the antenna gains for the ray depends on the antenna patterns and the angles between the ray and the boresights of the antennas. Real antenna patterns could of course be used, but for simplicity, the antenna patterns are approximated by sinc functions of the true angles between the ray and the boresights (sinc(x)=sin(x)/x). Then, only a boresight gain and beamwidth are necessary to define each antenna pattern. The antenna patterns are approximated by

$$G(\alpha_b) = G_o + 10\log(\mathrm{sinc}^2(K\alpha_b)), \tag{26}$$

where G_o is the gain of the antenna along the boresight, α_b is the true angle between the boresight and the ray, and K is a constant determining the beamwidth of the antenna. Suppose the antenna pattern to be approximated has a 3 dB beamwidth of B_w. Then because 20log(sinc(v)) = -3 dB when v = 1.39, $KB_w/2$ must equal 1.39, so that

$$K = 2.78/B_w. \tag{27}$$

The true angle, α_b, between the antenna boresight (having an azimuthal angle of B_a and elevation angle of B_e) and the ray, is found from (10) using the appropriate direction ratios. For the transmitter, the direction ratios are

$$A_1 = \cos(B_a)\cos(B_e), \tag{28a}$$

$$B_1 = \sin(B_a)\cos(B_e), \tag{28b}$$

$$C_1 = \sin(B_e), \tag{28c}$$

$$A_2 = \cos(\alpha_t)\cos(\beta_t), \tag{29a}$$

$$B_2 = \sin(\alpha_t)\cos(\beta_t), \tag{29b}$$

and

$$C_2 = \sin(\beta_t). \tag{29c}$$

For the receiver, the first three direction ratios are given by (28) where Ba and Be are now the azimuthal and elevation angles of the boresight of the receiving antenna. The last three direction ratios for the receiver are given by

$$A_2 = \cos(\alpha_r)\cos(\beta_r), \tag{30a}$$

$$B_2 = \sin(\alpha_r)\cos(\beta_r), \tag{30b}$$

and

$$C_2 = \sin(\beta_r). \tag{30c}$$

For the idealized physical model, separate, but constant, values for the coefficients of reflection are used for the walls and street. The phase of the reflection coefficients is assumed to be 180 degrees. The magnitude is treated as a loss given in dB. The total loss in dB due to reflections is then given by the wall reflection loss multiplied by the number of wall reflections plus the street reflection loss, if there is a street reflection. With the wall and street reflection losses given in dB by C_w and C_s, respectively, the loss due to reflection is

$$L_r = |N|C_w + u(-M)C_s, \tag{31}$$

where again u(•) is the unit step function as defined above.

The clear-air absorption loss is

$$L_a = \alpha_a L, \tag{32}$$

where L is the length of the ray and α_a is the attenuation rate in dB/km as computed based on the model of Liebe (1985).

3.2.3 Ray phase

The phase of each ray is determined by its length and its reflection from the walls and street. The ray phase at the receiver is given by

$$\theta = 2\pi L/\lambda + \pi(|N| + u(-M)), \tag{33}$$

where a phase shift of π has been assumed for each reflection.

3.2.4 Received signal level

The signal at the receiver is modeled as consisting of the sum of all the possible rays from the transmitter to the receiver. In (24), the ray amplitude, A, is given in dBm (at the output of the receiving antenna). In order to sum the rays, the amplitude of each ray in linear units is needed. Here, it is sufficient to give the amplitude, a, in arbitrary linear units. These two measures of ray amplitude are related by

$$A = 20\log(a) \tag{34}$$

and

$$a = 10^{A/20}. \tag{35}$$

Using (24), (33), and (35) the rays may be summed as

$$S = \sum a_{N,M}\exp(-j\theta_{N,M}). \tag{36}$$

The received signal amplitude in dBm is then

$$A_s = 20\log(|S|). \tag{37}$$

3.2.5 Effect of variations in building walls

Variations in the building walls such as differences in building materials, surface roughness, windows and doors, etc., will in the real world cause the reflection coefficient for the walls to vary along the street. This variation is not accounted for in the above model for the ray amplitude. These same features will also cause scattering and diffraction of the millimeter waves into the receiving antenna as will other objects in the vicinity. These effects are not included in the model but more will be said about them below.

In Figure 1, it can be seen that the variation in the distance of the buildings from the street center becomes geometrically insignificant after a few blocks. Therefore, the angles of the rays in the idealized environment should not differ significantly from the angles in a real street. However, a reflection in the real world depends on a surface area and does not occur at a single point as specular reflection has been modeled here. The active reflecting surface can be divided into Fresnel zones about the point of specular reflection (Beckmann and Spizzichino, 1963). The first Fresnel zone is bounded by the ellipse of reflection points whose total path delay between the transmitter and receiver differs by $\lambda/2$ from the specular path. The reflected field is normally found by integrating over the first few Fresnel zones. These Fresnel zones of reflection would have a large horizontal extent encompassing a great deal of surface roughness when the path is several blocks long. The surface variation within the Fresnel zones can be thought of as affecting the phase and amplitude of the reflected ray but not significantly altering the geometry of its reflection. Indeed, the gaps in the walls due to cross streets can also be considered to modulate the phase and amplitude of the reflected ray.

The reflection coefficient for a smooth surface is known to be a function of the angle of incidence and the polarization (Rice et al., 1967). The "Brewster" angle effect can cause a significant difference in the value of the reflection coefficient between vertical and horizontal polarizations. This effect has not been included in the model for several reasons. First, it applies to smooth surfaces while the building walls are irregular. Secondly, the irregularities result in variations in the reflection coefficients that would overwhelm the "Brewster" angle effects. Thirdly, the Brewster angle would be expected to be greater than most of the angles of incidence for a typical urban path (except for paths less than about two hundred meters in length or ray paths with many wall reflections).

3.2.6 Cumulative distribution of received signal amplitude

The model, as it has been developed above, predicts a single value for received signal amplitude based on the summation of a number of ray paths between the transmitter and receiver as determined by the link geometry. Of course, as discussed above, the variations in the walls of a real street would result in unique ray phases and amplitudes that would cause the received signal level to deviate significantly from that predicted by the idealized model. The signal level predicted from the idealized model is not even the expected value

of the received signal level; it is a unique value determined by the particular phases and amplitudes of the summed rays. At best, it could be hoped that it would behave similarly, in a qualitative sense, to real received signal levels as a function of receiver location, frequency, etc.

Because the propagation situation of a real street would be so complex that it is not practical to predict an exact received signal level for arbitrary locations of the transmitter and receiver, it is desirable to predict the cumulative distribution of the signal level for an ensemble of real streets. That is, for all streets of a particular approximate width, what would be the distribution of the received signal level as the transmitter and receiver are moved from street to street, maintaining the same link geometry within the streets? Equivalently, what would be the distribution of the received signal level if the transmitter and receiver were kept in the same relative position to each other and the sides of the street, but were moving down the street? This sort of statistical estimate of the received signal level can be made using the idealized model.

Some information about the relative phase of the rays can be retained and therefore improve the estimate of the signal level. In particular, since the surfaces of many streets are rather uniform and in many places approximately flat, the prediction by the idealized model of the relative amplitude and phase of the direct line-of-sight ray and street-reflected ray is accurate for many real world scenarios. Therefore, the sum of these two rays is treated as a known component of the received signal.

Next, it is assumed that the relative phase of the wall-reflected rays is uniformly distributed from 0 to 2π because of the random deviation of real building walls from the idealized geometry. In addition, it is assumed that the summation of these rays is not dominated by any one ray. That is, although the amplitudes of the rays are random, no one ray has an amplitude so large that it unduly influences the sum. Then the magnitude or amplitude of the sum of the wall-reflected rays has a Rayleigh distribution.

The Rayleigh distribution is named after Lord Rayleigh (1894) who first derived it for the sum of a number of waves with independent uniformly distributed phase. The Rayleigh distribution is given by

$$p(|S_w| < z) = 1 - \exp(-z^2/\bar{a}_w^2), \qquad z > 0, \tag{38}$$

where $|S_w|$ is the amplitude and $\bar{a}_w^2$ is the average power of the sum of the wall-reflected rays. The average power of the sum is the sum of the powers of the wall reflected rays given by

$$\bar{a}_w^2 = \sum_{M,N \neq 0} a_{M,N}^2. \tag{39}$$

Converting to decibels by using

$$A_w = 20\log(|S_w|), \tag{40}$$

and substituting for the amplitude in the complement of (38) gives the complementary Rayleigh decibel distribution,

$$p(A_w > Z) = \exp(-10^{Z/10}/\bar{a}_w^2), \tag{41}$$

which gives the probability that the received signal amplitude in dB will be greater than Z. It is convenient to solve (41) for Z in terms of p giving the quantile

$$Z(p) = 10\log(-\ln(p)) + 10\log(\bar{a}_w^2), \tag{42}$$

so that the signal level exceeded p fraction of the time can be determined. This equation is especially convenient for computing mean and median signal levels and confidence intervals. The second term on the right hand side of (42) is the average power in dBm and is exceeded 1/e (≈ 0.368) fraction of the time. The median signal level is exceeded one-half the time and from (42) is found to be 1.59 dB less than the average signal level.

The received signal can now be estimated as the sum of a known or constant component (direct plus street reflected ray) and a Rayleigh distributed component (wall-reflected rays). The distribution of a constant plus a Rayleigh distributed component is known as the Nakagami-Rice or Ricean distribution (Nakagami, 1940 and Rice, 1945). There is one parameter, C, for the Nakagami-Rice distribution. This parameter is the ratio in dB of the power in the constant component to the average power in the Rayleigh component. When $C = -\infty$, the distribution is Rayleigh. When $C = +\infty$, the received signal

is a constant. The Nakagami-Rice distribution normalized to the median is shown plotted on "Rayleigh paper" in Figure 5.

The power in the known component (direct and street reflected ray) of the signal is

$$a_c^2 = |a_{0,1}\exp(-j\theta_{0,1}) + a_{0,-1}\exp(-j\theta_{0,-1})|^2. \tag{43}$$

The parameter C is then given by

$$C = 20\log(a_c/\bar{a}_w). \tag{44}$$

Because the computation of the Nakagami-Rice distribution involves the evaluation of Bessel functions and it depends on the parameter C in a nontrivial way, a convenient approximation is desirable. As can be seen in Figure 5, the Nakagami-Rice distribution is approximately a straight line on Rayleigh paper with its slope depending on the parameter C. The Weibull distribution (Weibull, 1951) plots as a straight line on Rayleigh paper with an arbitrary slope equal to $-\alpha$, where α is a parameter of the distribution. Therefore, the Weibull distribution can be used to approximate the Nakagami-Rice distribution (at least over the range of probabilities from 0.001 to 0.999).

Because on Rayleigh paper, the Rayleigh distribution is a straight line with a slope of -1 and the Weibull distribution is a straight line with slope $-\alpha$, the quantiles of the Weibull decibel distribution are easily found from (42) to be

$$Z(p) = \alpha 10\log(-\ln(p)) + 10\log(\bar{a}_w^2+a_c^2). \tag{45}$$

Notice that the median signal level is now 1.59α dB less than the average signal level which is the sum of the power in the random and constant components.

To approximate the distribution of the signal level by the Weibull distribution, the nontrival relationship between α and C must be known. Although, the relationship between α and C could be derived by matching the standard deviation or variance of the Weibull and Nakagami-Rice distributions, the interdecile range is used here. The interdecile range, ΔZ, is the difference between the signal levels exceeded 0.1 and 0.9 portions of the time. The interdecile range of the Weibull distribution is easily found from (45) to be

$$\Delta Z_w = 13.3954\alpha. \tag{46}$$

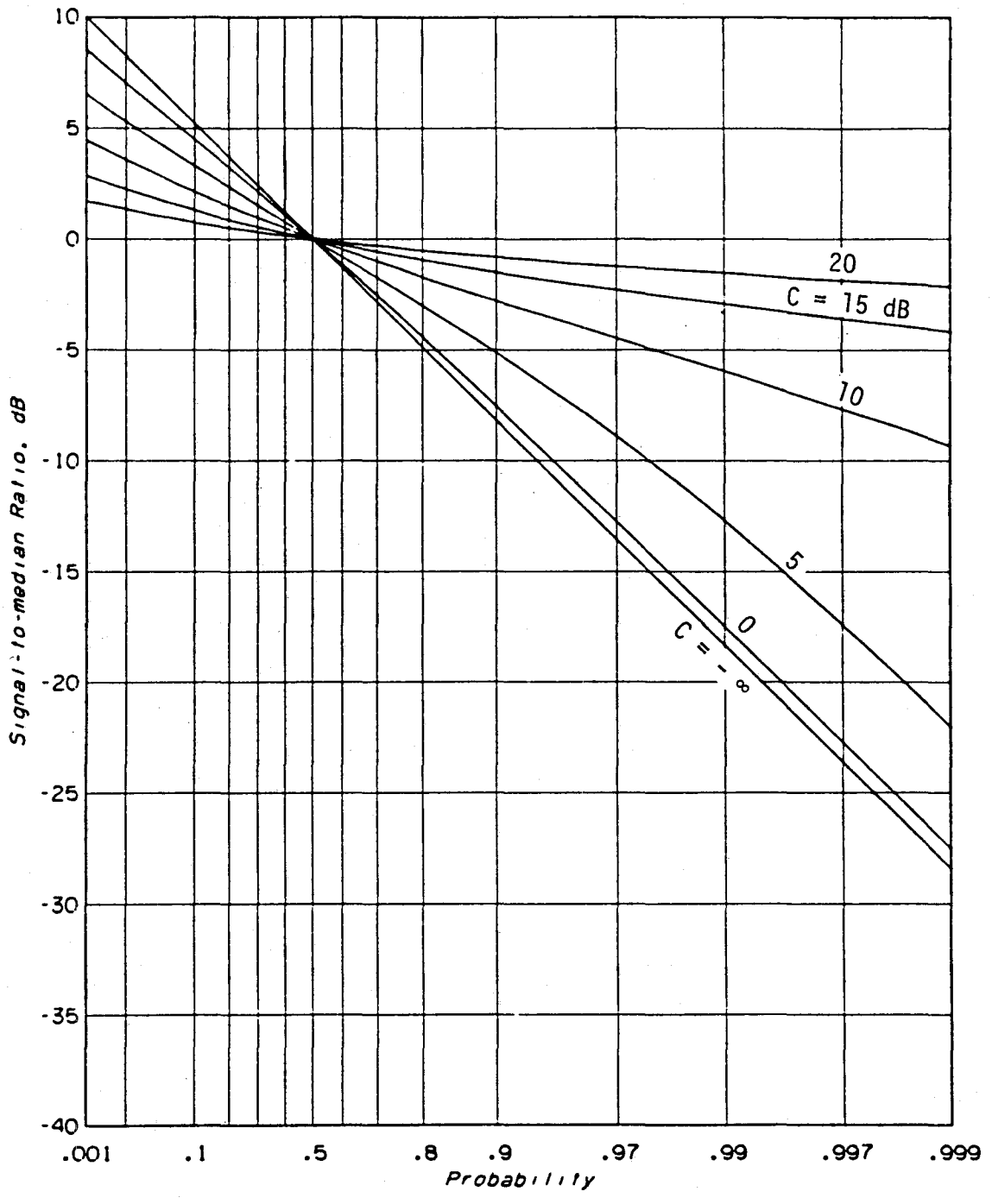

Figure 5. The Nakagami-Rice distribution (complement) on Rayleigh paper. The parameter C is the constant-to-scattered ratio in decibels.

The interdecile range for the Nakagami-Rice distribution has been given by Hufford and Ebaugh (1985) as shown in Figure 6. The values have also been given by Rice et al. (1967) and are presented in the table below.

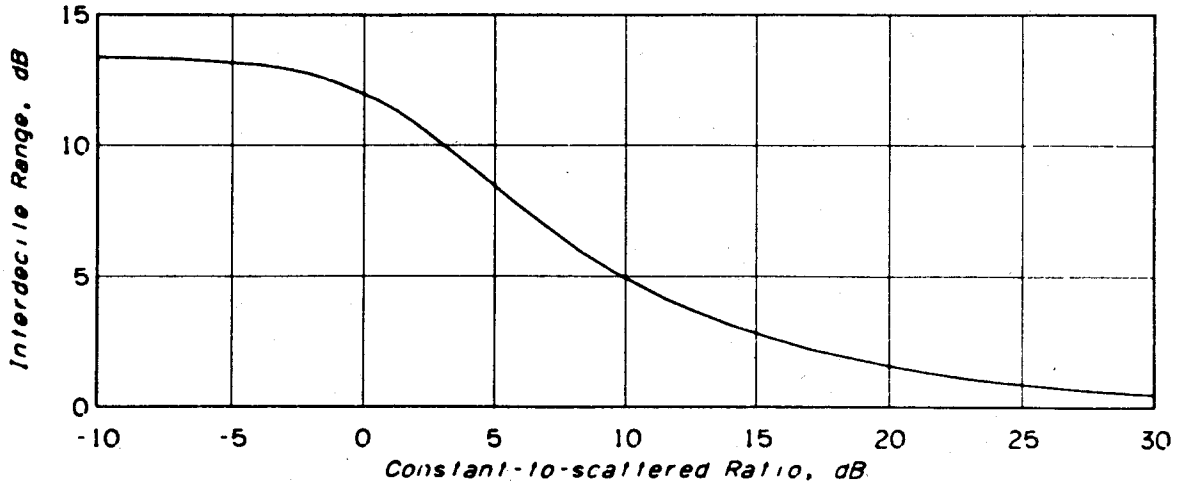

Figure 6. The interdecile range of the Nakagami-Rice distribution (Hufford and Ebaugh, 1985).

The interdecile range of the Nakagami-Rice distribution and the parameter C

C	ΔZ_N
$-\infty$	13.3954
-10	13.3729
-6	13.2619
0	12.0049
6	7.6021
10	4.9193
16	2.4884
20	1.5726
25	0.8850
30	0.4978
$+\infty$	0

A function fitting the values in the table giving ΔZ as a function of C is needed. It is convenient to choose the function

$$\Delta Z_N = 13.3954/(t + 1), \tag{47}$$

since it approaches 13.4 as t goes to zero, and 0 as t goes to $+\infty$. Now, t needs to be a function of C such that it goes to zero as C goes to $-\infty$ and it goes to $+\infty$ as C goes to $+\infty$. The function $t=\exp(C)$ satisfies this requirement, but a more complicated dependence on C can be achieved if $t=\exp(g(C))$ is used, where g is a function such that as C approaches + or $-\infty$, g also goes to + or $-\infty$, respectively. A polynomial of odd order with a positive coefficient for the highest power term satisfies this requirement. The value of the constant term of the polynomial is found to be -2.15565 from (47) using the value of ΔZ_N at $C=0$. A third order polynomial such that

$$t = \exp(g_0 + g_1 C + g_2 C^2 + g_3 C^3), \tag{48a}$$

was used to fit (46) to the data in the table with a resulting root-mean-square error of about 0.002 dB for the interdecile range with the coefficient values

$$g_0 = -2.1556515, \tag{48b}$$

$$g_1 = 0.3811766, \tag{48c}$$

$$g_2 = -0.01295302, \tag{48d}$$

and

$$g_3 = 2.145651\ X\ 10^{-4}. \tag{48e}$$

Using (46) and (47) then gives

$$\alpha = 1/(t + 1), \tag{49}$$

where $t(C)$ is defined by (48). This completes the information necessary to use the Weibull

distribution to estimate the statistics of the received signal amplitude for an ensemble of streets.

It is important to note that the average power in (39) is computed for the idealized model in which the loss due to a wall reflection is constant for each reflection. However, in the real world each reflection will have a different coefficient of reflection and some reflections will be so poor that the ray will be completely lost. The question immediately arises of how to estimate the power in the Rayleigh component when the reflection loss varies from reflection to reflection in the real world. It is the average power of the sum of the rays reflected from the real walls that is needed to compute C and predict the statistics of a signal in the real world. Fortunately, it can be assumed that the reflection losses are statistically independent because of surface irregularities. Then, it is straightforward to show that if the constant reflection loss, C_w, equals the average reflection loss of the real street, the average power computed in (39) equals the average power of the sum of the wall-reflected waves in the real street. In this case, the distribution as derived should give a good estimate of the expected signal level and confidence intervals when one knows beforehand the width of the street and the locations of the end terminals with respect to the building walls and each other.

4. COMPUTER MODEL CAPABILITIES

The model developed in the previous section was encoded in FORTRAN to run on an HP 1000 computer and later on an IBM-PC compatible computer. The program begins with a menu that allows the user to select the particular output desired. The user then enters the parameter values needed for the chosen output. These inputs describe the street environment and equipment specifications.

Because each reflection decreases the amplitude of the ray, rays with many reflections can be neglected. The user chooses the maximum number of wall reflections for which ray paths should be computed. This maximum is the upper limit on the index N in the summation in (36). This maximum is limited to 10 by the computer program. If three reflections were chosen as the maximum, then 14 rays would be used. They are the direct line-of-sight ray, the ground reflected ray, three rays without a ground reflection that are reflected from the right wall first (1, 2, and 3 reflections), three more rays to the right with

ground reflections, and finally the rays reflected first from the left wall that correspond to the previous six rays reflected first from the right.

Although all six outputs of the program are described below, only two of these output types (range scan and angle scan) are used, for direct comparison with measured data in section 5.

4.1 Ray Table

The ray table output provides a way of examining the detailed information of each ray for a particular path geometry. Figure 7 is an example ray table output. The rays each have an index (*M*,*N*). The first index, *M*, denotes whether or not the ray is reflected from the ground on its path to the receiver. If *M* is -1, the ray is reflected from the ground. If *M* is 1, the ray is not reflected from the ground. The second index, *N*, denotes the number of reflections from the walls. If *N* is negative, the ray is reflected first from the left wall. Otherwise, the ray is reflected first from the right wall.

The ray table describes each ray that arrives at the receiver. The first piece of information listed is the ray length, which determines the free space and absorption losses as well as the delay time to the receiver. The table also describes the angles of departure and arrival at the respective antennas. These angles determine the antenna gain factor for the amplitude of the ray. The table also lists the angle of reflection from the street and from the buildings, as well as the geometric coordinates of each reflection location. The effect of cross streets is approximated by assuming that when a wall reflection is located at a cross street, there is no reflection and the ray is lost (goes down the cross street). In Figure 7, two rays are identified as having gone "down a cross street." In practice, this method of accounting for the effects of cross streets results in discontinuities in the received signal level. Ignoring the cross streets gives outputs that look more like measured data.

4.2 Range Scan

The range scan output mode predicts the distance dependence of the received signal level. The receiver is moved back from the transmitter along the y-axis while the transmitter remains fixed. For each receiver location, the computer calculates the ray paths between the transmitter and the receiver. Received signal level is plotted in dBm versus

SUMMARY OF PARAMETERS

Index	Description	Value
1.	Maximum number of wall reflections (integer)	2.000
2.	Distance between building walls (m)	24.000
3.	TX distance from left wall (m)	5.000
5.	TX height from street (m)	2.150
6.	RX distance from right wall (m)	5.000
7.	RX distance from TX (m)	100.000
11.	RX height from street (m)	1.800
43.	Are cross streets to be used (1=yes,0=no)	1.000
44.	Distance from TX to first cross street (m)	10.000
45.	Distance between cross streets (m)	76.000
46.	Width of cross street (m)	24.000
47.	Plot distribution: (0=no, 1=yes)	0.000
48.	Plot distribution separately: (0=no, 1=yes)	1.000
49.	Plot actual value: (0=no, 1=yes)	1.000
50.	Confidence interval (decimal)	0.900

TABLE OF RAY PATHS

RAY INDEX: -1,-2 Ray Length: 110.994
Transmitter: Azimuth= -25.641 Elevation= -2.039
Receiver : Azimuth= -25.641 Elevation= -2.039
Angle of reflection from buildings= 25.623
Angle of reflection from street= 2.039
Locations of reflection points:

X	Y	Z
0.00	10.42	1.74
24.00	60.42	0.24
21.13	54.43	0.00

THIS RAY WENT DOWN A CROSS STREET.

RAY INDEX: -1,-1 Ray Length: 100.576
Transmitter: Azimuth= -5.711 Elevation= -2.251
Receiver : Azimuth= 5.711 Elevation= -2.251
Angle of reflection from buildings= 5.706
Angle of reflection from street= 2.251
Locations of reflection points:

X	Y	Z
0.00	50.00	0.18
0.44	54.43	0.00

RAY INDEX: -1, 0 Ray Length: 100.078
Transmitter: Azimuth= 0.000 Elevation= -2.262
Receiver : Azimuth= 0.000 Elevation= -2.262
Angle of reflection from street= 2.262
Locations of reflection points:

X	Y	Z
5.00	54.43	0.00

RAY INDEX: -1, 1 Ray Length: 107.050
Transmitter: Azimuth= 20.807 Elevation= -2.115
Receiver : Azimuth= -20.807 Elevation= -2.115
Angle of reflection from buildings= 20.792
Angle of reflection from street= 2.114
Locations of reflection points:

X	Y	Z
24.00	50.00	0.18
22.32	54.43	0.00

RAY INDEX: -1, 2 Ray Length: 110.994
Transmitter: Azimuth= 25.641 Elevation= -2.039
Receiver : Azimuth= 25.641 Elevation= -2.039
Angle of reflection from buildings= 25.624
Angle of reflection from street= 2.039
Locations of reflection points:

X	Y	Z
24.00	39.58	0.59
0.00	89.58	1.39
16.87	54.43	0.00

RAY INDEX: 1,-2 Ray Length: 110.924
Transmitter: Azimuth= -25.641 Elevation= -0.181
Receiver : Azimuth= -25.641 Elevation= 0.181
Angle of reflection from buildings= 25.641
Locations of reflection points:

X	Y	Z
0.00	10.42	2.11
24.00	60.42	1.94

THIS RAY WENT DOWN A CROSS STREET.

RAY INDEX: 1,-1 Ray Length: 100.499
Transmitter: Azimuth= -5.711 Elevation= -0.200
Receiver : Azimuth= 5.711 Elevation= 0.200
Angle of reflection from buildings= 5.710
Locations of reflection points:

X	Y	Z
0.00	50.00	1.98

RAY INDEX: 1, 0 Ray Length: 100.001
Transmitter: Azimuth= 0.000 Elevation= -0.201
Receiver : Azimuth= 0.000 Elevation= 0.201
LINE OF SIGHT RAY

RAY INDEX: 1, 1 Ray Length: 106.977
Transmitter: Azimuth= 20.807 Elevation= -0.187
Receiver : Azimuth= -20.807 Elevation= 0.187
Angle of reflection from buildings= 20.807
Locations of reflection points:

X	Y	Z
24.00	50.00	1.98

RAY INDEX: 1, 2 Ray Length: 110.924
Transmitter: Azimuth= 25.641 Elevation= -0.181
Receiver : Azimuth= 25.641 Elevation= 0.181
Angle of reflection from buildings= 25.641
Locations of reflection points:

X	Y	Z
24.00	39.58	2.01
0.00	89.58	1.84

Figure 7. An example of the ray table output with input parameter list.

distance in meters. Figure 8 is an example of a range scan output. Expected signal level and confidence intervals using the Weibull distribution are also available versus distance.

4.3 Frequency Scan

The frequency scan mode predicts the received signal level as a function of frequency. Both the receiver and the transmitter remain in fixed positions. The computer calculates the signal level over a user-defined frequency interval. Zero bandwidth is assumed. Because the relative phase of the rays depends on the frequency, the signal level varies with frequency. A plot of signal level versus frequency is shown in Figure 9. Again, expected signal level and confidence intervals are available.

4.4 Angle Scan

The signal level as a function of either the azimuth or elevation angle of the receiving antenna is estimated. Like the frequency scan mode, the receiver and the transmitter locations remain fixed. The user defines the azimuth or elevation angle interval. The antenna gain for each ray changes as a function of the antenna angle. The output is a plot of the received signal level as a function of azimuth or elevation angle. Figure 10 depicts an azimuth angle scan output. Again, expected signal level and confidence intervals are also available.

4.5 Angles of Arrival

The angle-of-arrival mode shows the angles of arrival at the receiver and the relative strengths of the rays. Both the transmitter and receiver remain fixed. The output consists of dots on the azimuth-elevation plane representing the rays. The relative size of the dots gives the relative amplitude of the rays. The computer can calculate the ray amplitudes with or without the effect of the antenna gains. Figure 11 shows the angle-of-arrival plots with antenna gains included. The plot shows the effects of the antenna pointing.

The angle-of-arrival plot can be used to adjust antenna pointing in the field. The plot indicates where to look for possible rays. Especially in the case of narrowbeam antennas, this information makes maximization of the received signal level possible as well as aiding in the avoidance of undesirable multipath components.

SUMMARY OF PARAMETERS

Index	Description	Value
1.	Maximum number of wall reflections (integer)	4.000
2.	Distance between building walls (m)	24.000
3.	TX distance from left wall (m)	5.000
5.	TX height from street (m)	2.150
6.	RX distance from right wall (m)	5.000
8.	Minimum distance from TX to RX (m)	50.000
9.	Maximum distance from TX to RX (m)	950.000
10.	Step size in distance from TX to RX (m)	1.000
11.	RX height from street (m)	1.800
12.	Radio Frequency (GHz)	28.800
16.	TX ant. beamwidth (degrees)	30.000
17.	TX antenna gain (dB)	17.000
18.	TX ant. elevation angle (degrees)	0.000
22.	TX ant. azmuthal angle (left-neg., degrees)	0.000
26.	RX ant. beamwidth (degrees)	2.400
27.	RX antenna gain (dB)	17.000
28.	RX ant. elevation angle (degrees)	0.000
32.	RX ant. azmuthal angle (left-neg., degrees)	0.000
36.	Transmitter power (dBm)	18.500
38.	Loss for street reflection (dB)	1.000
39.	Loss for wall reflection (dB)	1.000
40.	Atmospheric Pressure (kPa)	83.000
41.	Relative Humidity (Percent)	50.000
42.	Temperature (Celsius)	20.000
43.	Are cross streets to be used (1=yes,0=no)	0.000
44.	Distance from TX to first cross street (m)	10.000
45.	Distance between cross streets (m)	76.000
46.	Width of cross street (m)	24.000
47.	Plot distribution: (0=no, 1=yes)	0.000
48.	Plot distribution separately: (0=no, 1=yes)	1.000
49.	Plot actual value: (0=no, 1=yes)	1.000
50.	Confidence interval (decimal)	0.900

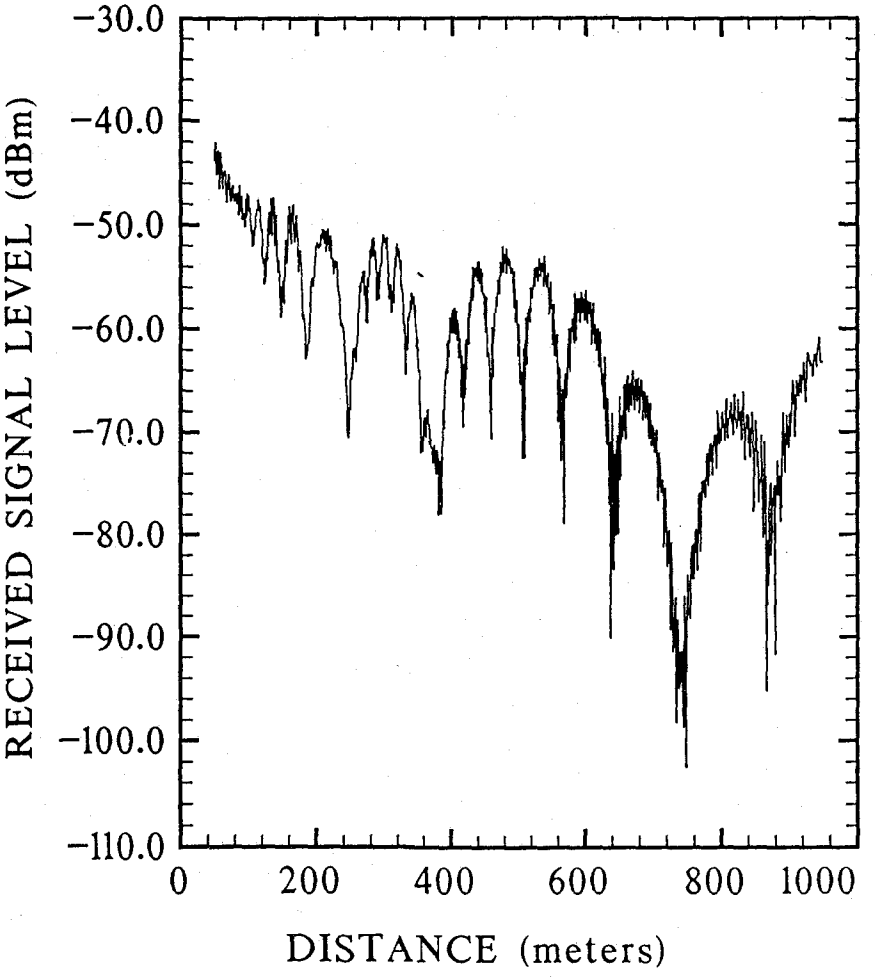

Figure 8. An example of range scan output with input parameter list.

SUMMARY OF PARAMETERS

Index	Description	Value
1.	Maximum number of wall reflections (integer)	4.000
2.	Distance between building walls (m)	24.000
3.	TX distance from left wall (m)	5.000
5.	TX height from street (m)	2.150
6.	RX distance from right wall (m)	5.000
7.	RX distance from TX (m)	500.000
11.	RX height from street (m)	1.800
13.	Minimum radio frequency (GHz)	10.000
14.	Maximum radio frequency (GHz)	60.000
15.	Step in radio frequency (GHz)	0.100
16.	TX ant. beamwidth (degrees)	30.000
17.	TX antenna gain (dB)	17.000
18.	TX ant. elevation angle (degrees)	0.000
22.	TX ant. azmuthal angle (left-neg., degrees)	0.000
26.	RX ant. beamwidth (degrees)	2.400
27.	RX antenna gain (dB)	17.000
28.	RX ant. elevation angle (degrees)	0.000
32.	RX ant. azmuthal angle (left-neg., degrees)	0.000
36.	Transmitter power (dBm)	18.500
38.	Loss for street reflection (dB)	1.000
39.	Loss for wall reflection (dB)	1.000
40.	Atmospheric Pressure (kPa)	83.000
41.	Relative Humidity (Percent)	50.000
42.	Temperature (Celsius)	20.000
43.	Are cross streets to be used (1=yes,0=no)	0.000
44.	Distance from TX to first cross street (m)	10.000
45.	Distance between cross streets (m)	76.000
46.	Width of cross street (m)	24.000
47.	Plot distribution: (0=no, 1=yes)	0.000
48.	Plot distribution separately: (0=no, 1=yes)	1.000
49.	Plot actual value: (0=no, 1=yes)	1.000
50.	Confidence interval (decimal)	0.900

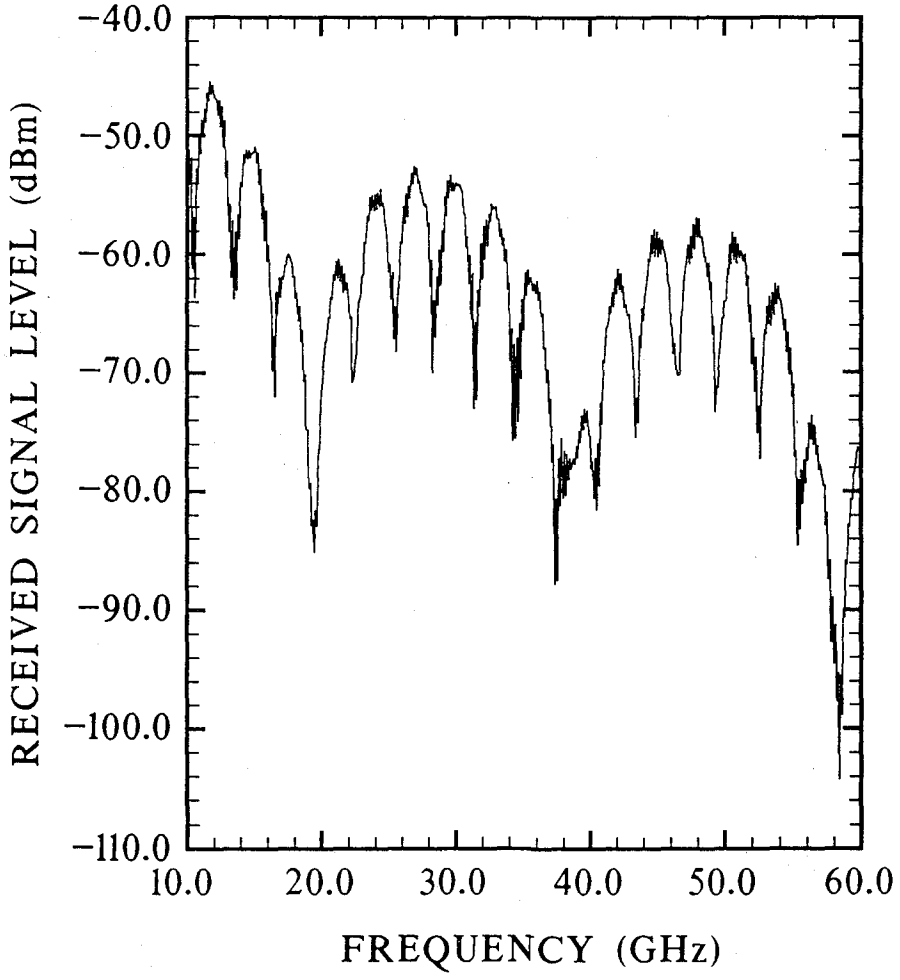

Figure 9. An example of a frequency scan output and input parameter list.

SUMMARY OF PARAMETERS

Index	Description	Value
1.	Maximum number of wall reflections (integer)	4.000
2.	Distance between building walls (m)	24.000
3.	TX distance from left wall (m)	5.000
5.	TX height from street (m)	2.150
6.	RX distance from right wall (m)	5.000
7.	RX distance from TX (m)	200.000
11.	RX height from street (m)	1.800
12.	Radio Frequency (GHz)	28.800
16.	TX ant. beamwidth (degrees)	30.000
17.	TX antenna gain (dB)	17.000
22.	TX ant. azmuthal angle (left-neg., degrees)	0.000
26.	RX ant. beamwidth (degrees)	2.400
27.	RX antenna gain (dB)	17.000
28.	RX ant. elevation angle (degrees)	0.000
29.	Minimum RX elevation angle (degrees)	-5.000
30.	Maximum RX elevation angle (degrees)	5.000
31.	Step size in RX elevation angle (degrees)	0.010
32.	RX ant. azmuthal angle (left-neg., degrees)	0.000
33.	Minimum RX azmuthal angle (degrees)	-30.000
34.	Maximum RX azmuthal angle (degrees)	30.000
35.	Step size in RX azmuthal angle (degrees)	0.100
36.	Transmitter power (dBm)	18.500
37.	Receiver noise figure (dB)	6.000
38.	Loss for street reflection (dB)	1.000
39.	Loss for wall reflection (dB)	1.000
40.	Atmospheric Pressure (kPa)	83.000
41.	Relative Humidity (Percent)	50.000
42.	Temperature (Celsius)	20.000
43.	Are cross streets to be used (1=yes,0=no)	0.000
44.	Distance from TX to first cross street (m)	10.000
45.	Distance between cross streets (m)	76.000
46.	Width of cross street (m)	24.000
47.	Plot distribution: (0=no, 1=yes)	0.000
48.	Plot distribution separately: (0=no, 1=yes)	0.000
49.	Plot actual value: (0=no, 1=yes)	1.000
50.	Confidence interval (decimal)	0.900

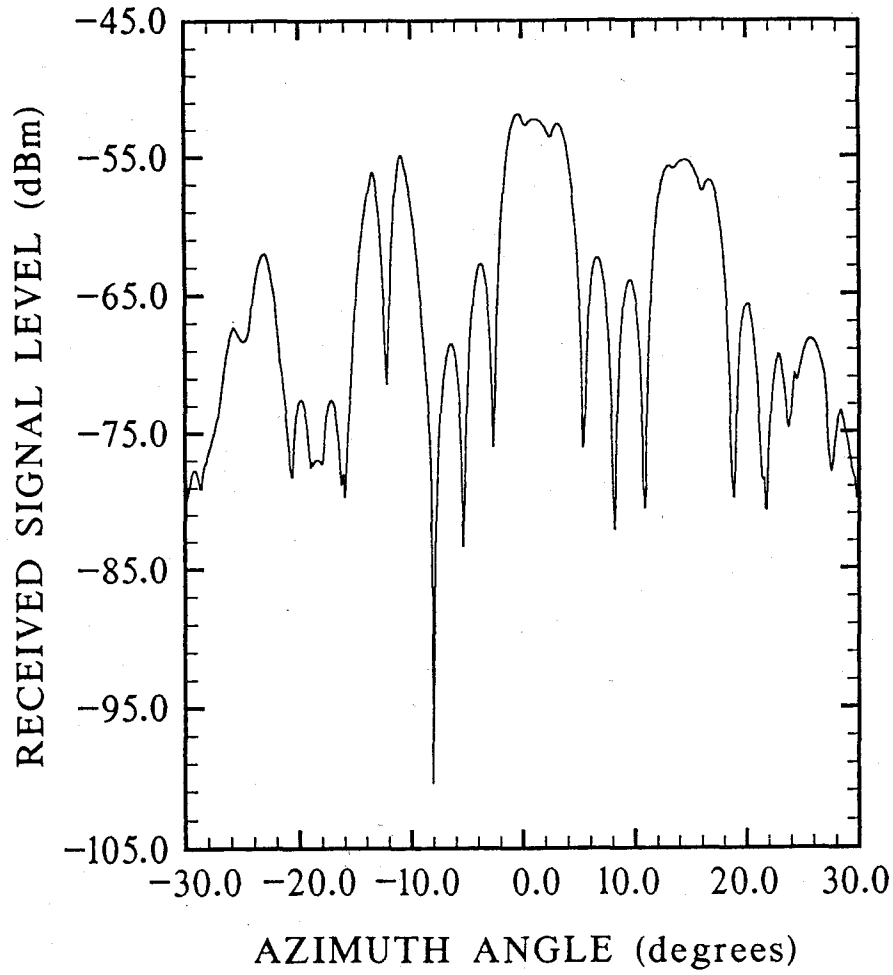

Figure 10. An example of an azimuth-angle scan and input parameter list.

SUMMARY OF PARAMETERS

Index	Description	Value
1.	Maximum number of wall reflections (integer)	4.000
2.	Distance between building walls (m)	24.000
3.	TX distance from left wall (m)	5.000
5.	TX height from street (m)	2.150
6.	RX distance from right wall (m)	5.000
7.	RX distance from TX (m)	200.000
11.	RX height from street (m)	1.800
12.	Radio Frequency (GHz)	28.800
16.	TX ant. beamwidth (degrees)	30.000
17.	TX antenna gain (dB)	17.000
22.	TX ant. azmuthal angle (left-neg., degrees)	0.000
26.	RX ant. beamwidth (degrees)	2.400
27.	RX antenna gain (dB)	17.000
28.	RX ant. elevation angle (degrees)	0.000
29.	Minimum RX elevation angle (degrees)	-5.000
30.	Maximum RX elevation angle (degrees)	5.000
31.	Step size in RX elevation angle (degrees)	0.010
32.	RX ant. azmuthal angle (left-neg., degrees)	0.000
33.	Minimum RX azmuthal angle (degrees)	-30.000
34.	Maximum RX azmuthal angle (degrees)	30.000
35.	Step size in RX azmuthal angle (degrees)	0.100
36.	Transmitter power (dBm)	18.500
37.	Receiver noise figure (dB)	6.000
38.	Loss for street reflection (dB)	1.000
39.	Loss for wall reflection (dB)	1.000
40.	Atmospheric Pressure (kPa)	83.000
41.	Relative Humidity (Percent)	50.000
42.	Temperature (Celsius)	20.000
43.	Are cross streets to be used (1=yes,0=no)	0.000
44.	Distance from TX to first cross street (m)	10.000
45.	Distance between cross streets (m)	100.000
46.	Width of cross street (m)	10.000
47.	Plot distribution: (0=no, 1=yes)	1.000
48.	Plot distribution separately: (0=no, 1=yes)	1.000
49.	Plot actual value: (0=no, 1=yes)	1.000
50.	Confidence interval (decimal)	0.900

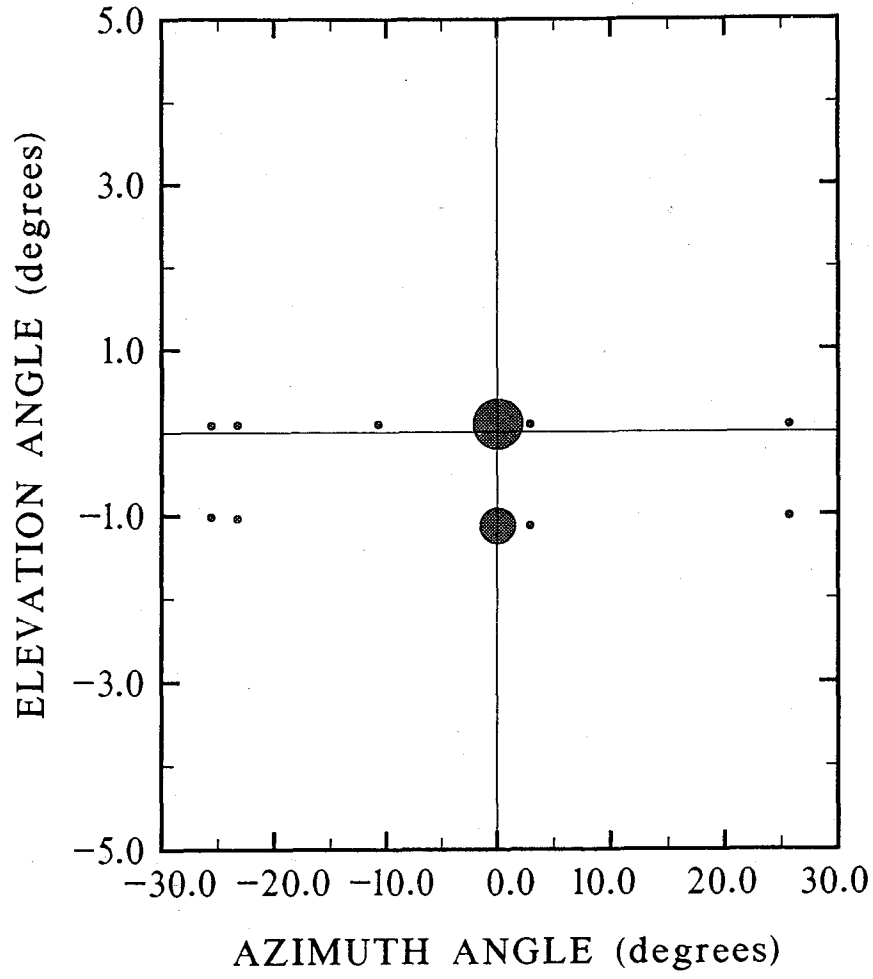

Figure 11. An example of the angle-of-arrival output and input parameter list.

4.6 Impulse Response

The impulse response mode plots the amplitude and delay time of the rays. The delay time of each ray is determined from the path length of the ray. The line-of-sight ray appears at time zero. All other rays appear at the time they are delayed relative to the line-of-sight ray. The computer plots the signal level relative to the line-of-sight ray. Figure 12 shows an impulse response plot.

4.7 Dependence of Model Predictions on Parameters

The four range scans in Figure 13 show the effect of the coefficients of reflection. The input parameters for Figure 13a are listed in Figure 14. In Figure 13a, the street-reflection and wall-reflection losses were set to 50 dB in order to effectively eliminate all reflections. The decreasing level with increasing distance results from free-space loss for the line-of-sight ray. The only input parameters changed in the remaining plots were the reflection losses. In Figure 13b, the street-reflection loss was set to 1 dB and the destructive interference of the line-of-sight ray and street-reflected ray can be seen. The dashed line is the line-of-sight ray amplitude. In Figure 13c, both the street- and wall-reflection losses are 1 dB. The interference pattern of all the components to the signal can be seen. In Figure 13d, the wall-reflection loss is increased to 6 dB and a decrease in the amplitude of the more rapid amplitude fluctuations can be seen relative to those in Figure 13c.

Several figures will be used to show the dependence on frequency as a parameter. In Figure 15, received signal level is shown as a function of frequency. A summary of the input parameters is shown in the same figure. The losses for street- and wall-reflection were both 50 dB. The free-space loss is again seen for the line-of-sight ray. An additional loss centered at 60 GHz is due to the complex of oxygen absorptions lines near that frequency. Perhaps a more realistic example of how signal level may depend on frequency is shown in Figure 16, where the losses are 1 and 3 dB for street and wall reflections, respectively.

A second set of outputs to emphasize frequency dependence is shown in Figure 17. The received signal level as a function of distance (range scans) at three frequencies is shown. The increase in the number of fades per-unit-distance is clear. A summary of the input parameters for Figure 17a is shown in Figure 18. Only the frequency is different for Figures 17b and 17c.

SUMMARY OF PARAMETERS

Index	Description	Value
1.	Maximum number of wall reflections (integer)	4.000
2.	Distance between building walls (m)	24.000
3.	TX distance from left wall (m)	5.000
5.	TX height from street (m)	2.150
6.	RX distance from right wall (m)	5.000
7.	RX distance from TX (m)	300.000
11.	RX height from street (m)	1.800
12.	Radio Frequency (GHz)	30.300
16.	TX ant. beamwidth (degrees)	30.000
17.	TX antenna gain (dB)	17.000
18.	TX ant. elevation angle (degrees)	0.000
22.	TX ant. azmuthal angle (left-neg., degrees)	0.000
26.	RX ant. beamwidth (degrees)	30.000
27.	RX antenna gain (dB)	17.000
28.	RX ant. elevation angle (degrees)	0.000
32.	RX ant. azmuthal angle (left-neg., degrees)	0.000
36.	Transmitter power (dBm)	18.500
37.	Receiver noise figure (dB)	6.000
38.	Loss for street reflection (dB)	1.000
39.	Loss for wall reflection (dB)	1.000
40.	Atmospheric Pressure (kPa)	83.000
41.	Relative Humidity (Percent)	50.000
42.	Temperature (Celsius)	20.000
43.	Are cross streets to be used (1=yes,0=no)	0.000
44.	Distance from TX to first cross street (m)	10.000
45.	Distance between cross streets (m)	76.000
46.	Width of cross street (m)	24.000

The line of sight ray is **** dBm.

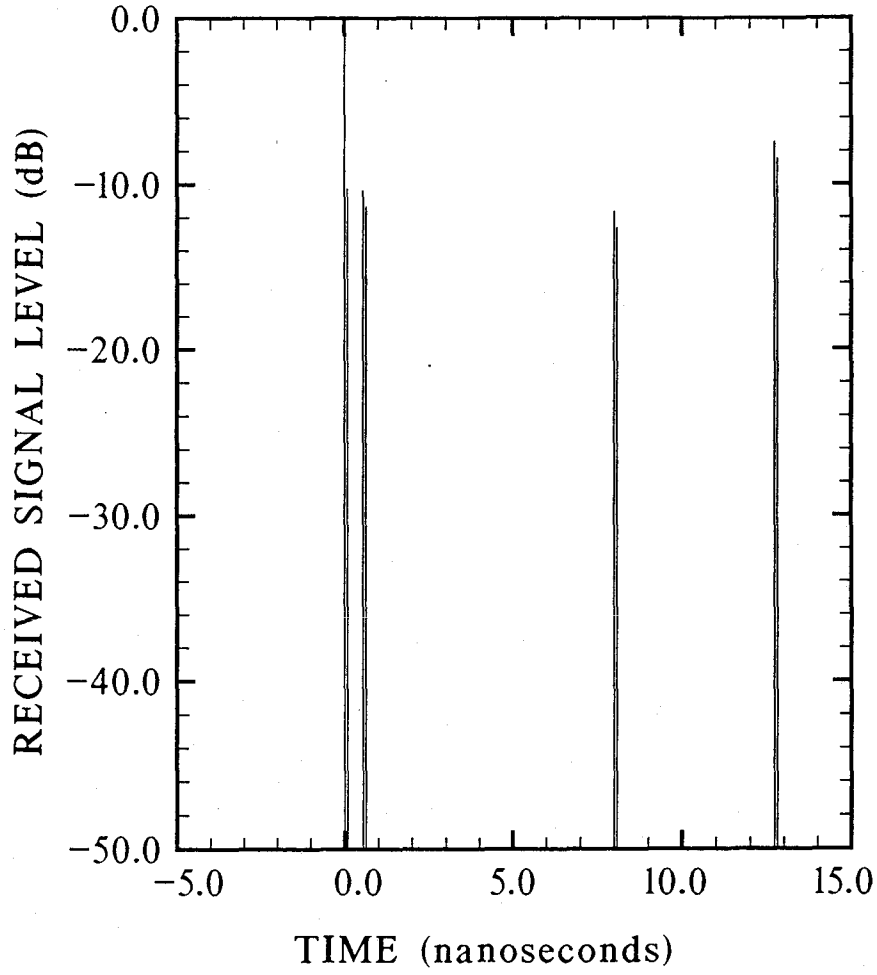

Figure 12. An example of an impulse-response output and input parameter list.

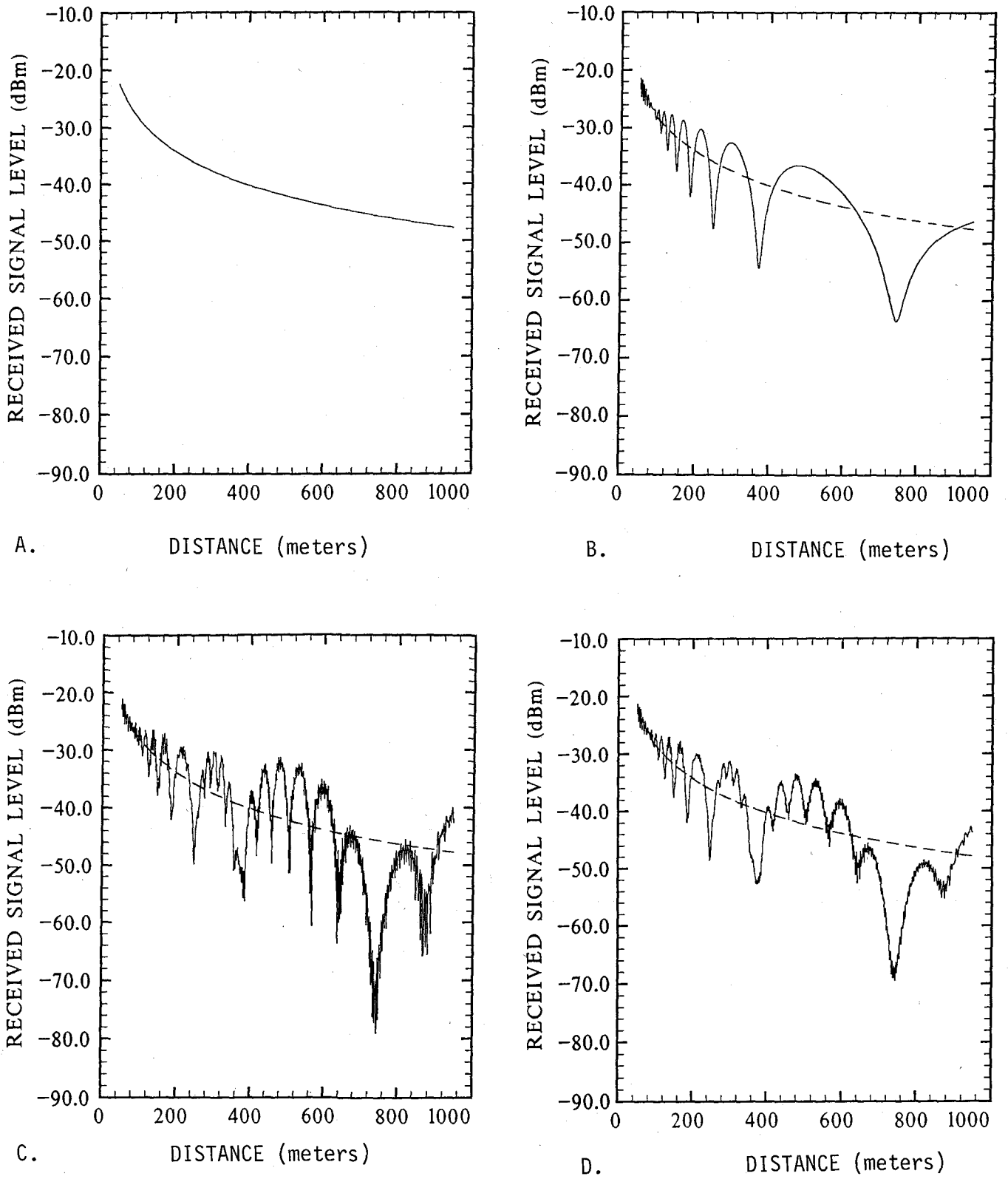

Figure 13. Four range scans showing variations due to differences in reflection losses.

SUMMARY OF PARAMETERS

Index	Description	Value
1.	Maximum number of wall reflections (integer)	3.000
2.	Distance between building walls (m)	24.000
3.	TX distance from left wall (m)	5.000
5.	TX height from street (m)	2.150
6.	RX distance from right wall (m)	5.000
8.	Minimum distance from TX to RX (m)	50.000
9.	Maximum distance from TX to RX (m)	950.000
10.	Step size in distance from TX to RX (m)	1.000
11.	RX height from street (m)	1.800
12.	Radio Frequency (GHz)	28.800
16.	TX ant. beamwidth (degrees)	30.000
17.	TX antenna gain (dB)	17.000
18.	TX ant. elevation angle (degrees)	0.000
22.	TX ant. azmuthal angle (left-neg., degrees)	0.000
26.	RX ant. beamwidth (degrees)	2.400
27.	RX antenna gain (dB)	38.000
28.	RX ant. elevation angle (degrees)	0.000
32.	RX ant. azmuthal angle (left-neg., degrees)	0.000
36.	Transmitter power (dBm)	18.500
38.	Loss for street reflection (dB)	50.000
39.	Loss for wall reflection (dB)	50.000
40.	Atmospheric Pressure (kPa)	83.000
41.	Relative Humidity (Percent)	50.000
42.	Temperature (Celsius)	20.000
43.	Are cross streets to be used (1=yes,0=no)	0.000
44.	Distance from TX to first cross street (m)	10.000
45.	Distance between cross streets (m)	76.000
46.	Width of cross street (m)	24.000
47.	Plot distribution: (0=no, 1=yes)	0.000
48.	Plot distribution separately: (0=no, 1=yes)	1.000
49.	Plot actual value: (0=no, 1=yes)	1.000
50.	Confidence interval (decimal)	0.900

Figure 14. The input parameter list for Figure 13a. Only the reflection losses are different for Figures 13b, 13c, and 13d.

SUMMARY OF PARAMETERS

Index	Description	Value
1.	Maximum number of wall reflections (integer)	4.000
2.	Distance between building walls (m)	24.000
3.	TX distance from left wall (m)	5.000
5.	TX height from street (m)	2.150
6.	RX distance from right wall (m)	5.000
7.	RX distance from TX (m)	500.000
11.	RX height from street (m)	1.800
13.	Minimum radio frequency (GHz)	5.000
14.	Maximum radio frequency (GHz)	80.000
15.	Step in radio frequency (GHz)	0.100
16.	TX ant. beamwidth (degrees)	30.000
17.	TX antenna gain (dB)	17.000
18.	TX ant. elevation angle (degrees)	0.000
22.	TX ant. azmuthal angle (left-neg., degrees)	0.000
26.	RX ant. beamwidth (degrees)	2.400
27.	RX antenna gain (dB)	38.000
28.	RX ant. elevation angle (degrees)	0.000
32.	RX ant. azmuthal angle (left-neg., degrees)	0.000
36.	Transmitter power (dBm)	18.500
38.	Loss for street reflection (dB)	50.000
39.	Loss for wall reflection (dB)	50.000
40.	Atmospheric Pressure (kPa)	83.000
41.	Relative Humidity (Percent)	50.000
42.	Temperature (Celsius)	20.000
43.	Are cross streets to be used (1=yes,0=no)	0.000
44.	Distance from TX to first cross street (m)	10.000
45.	Distance between cross streets (m)	76.000
46.	Width of cross street (m)	24.000
47.	Plot distribution: (0=no, 1=yes)	0.000
48.	Plot distribution separately: (0=no, 1=yes)	1.000
49.	Plot actual value: (0=no, 1=yes)	1.000
50.	Confidence interval (decimal)	0.900

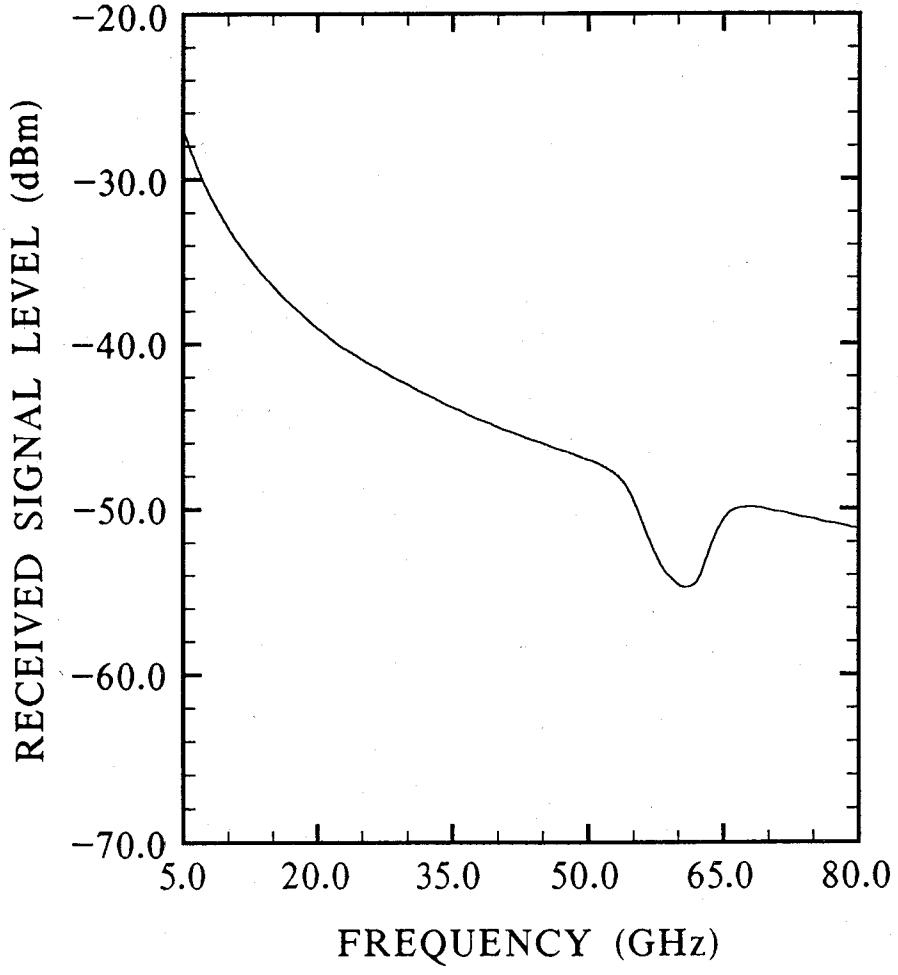

Figure 15. A frequency scan showing the effects of free-space loss and clear-air absorption.

SUMMARY OF PARAMETERS

Index	Description	Value
1.	Maximum number of wall reflections (integer)	4.000
2.	Distance between building walls (m)	24.000
3.	TX distance from left wall (m)	5.000
5.	TX height from street (m)	2.150
6.	RX distance from right wall (m)	5.000
7.	RX distance from TX (m)	500.000
11.	RX height from street (m)	1.800
13.	Minimum radio frequency (GHz)	10.000
14.	Maximum radio frequency (GHz)	60.000
15.	Step in radio frequency (GHz)	0.100
16.	TX ant. beamwidth (degrees)	30.000
17.	TX antenna gain (dB)	17.000
18.	TX ant. elevation angle (degrees)	0.000
22.	TX ant. azmuthal angle (left-neg., degrees)	0.000
26.	RX ant. beamwidth (degrees)	2.400
27.	RX antenna gain (dB)	38.000
28.	RX ant. elevation angle (degrees)	0.000
32.	RX ant. azmuthal angle (left-neg., degrees)	0.000
36.	Transmitter power (dBm)	18.500
38.	Loss for street reflection (dB)	1.000
39.	Loss for wall reflection (dB)	3.000
40.	Atmospheric Pressure (kPa)	83.000
41.	Relative Humidity (Percent)	50.000
42.	Temperature (Celsius)	20.000
43.	Are cross streets to be used (1=yes,0=no)	0.000
44.	Distance from TX to first cross street (m)	10.000
45.	Distance between cross streets (m)	76.000
46.	Width of cross street (m)	24.000
47.	Plot distribution: (0=no, 1=yes)	0.000
48.	Plot distribution separately: (0=no, 1=yes)	1.000
49.	Plot actual value: (0=no, 1=yes)	1.000
50.	Confidence interval (decimal)	0.900

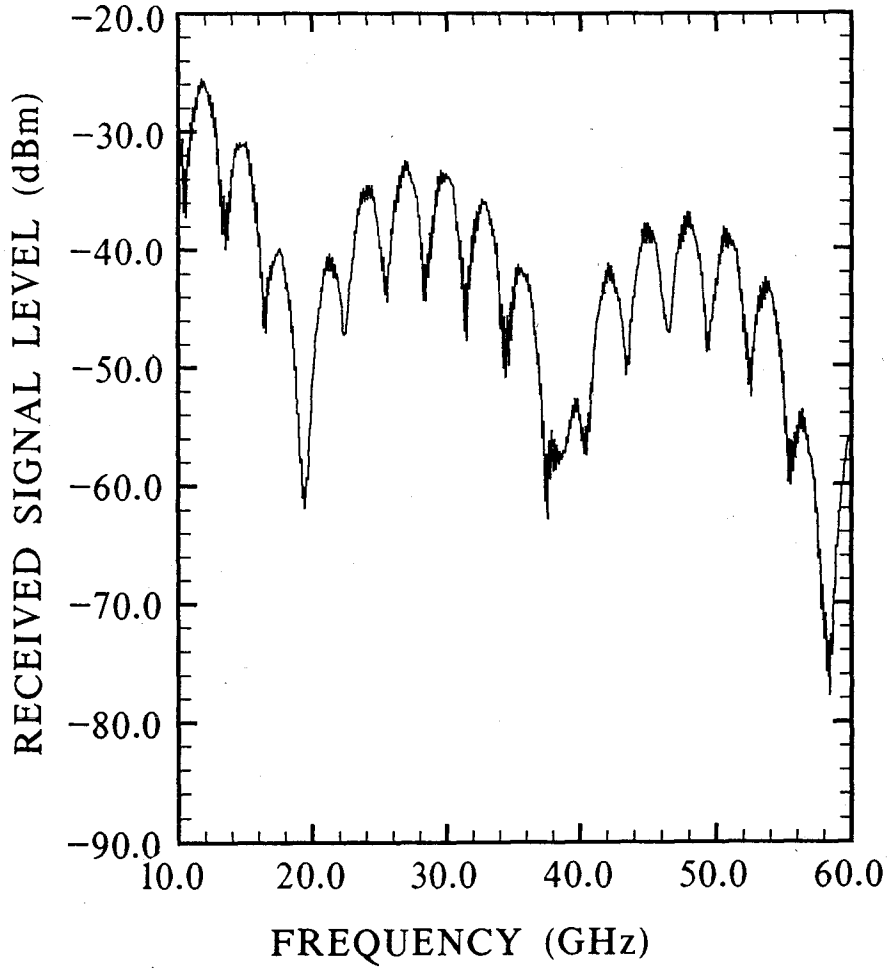

Figure 16. A frequency scan showing the effects of street- and wall-reflections and input parameter list.

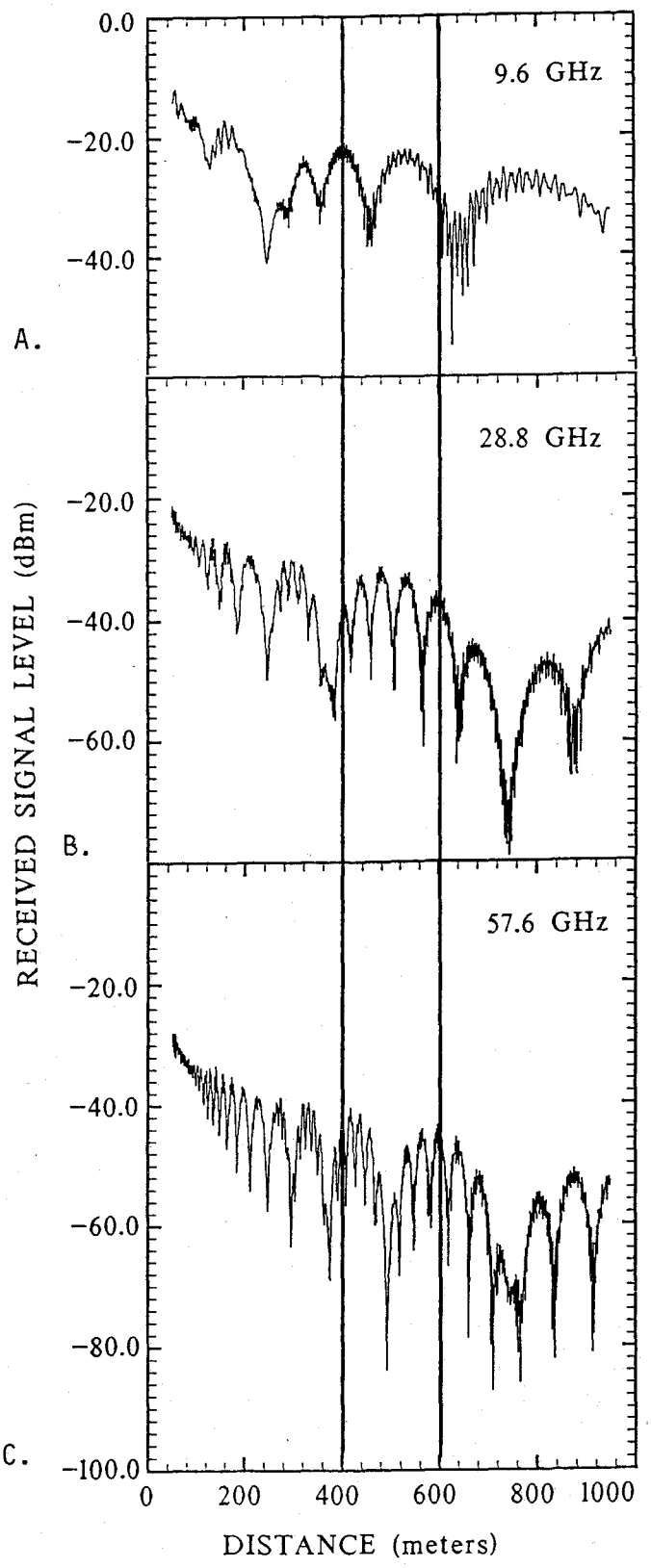

Figure 17. Range scans for several frequencies showing the dependence of the fading rate on frequency.

SUMMARY OF PARAMETERS

Index	Description	Value
1.	Maximum number of wall reflections (integer)	3.000
2.	Distance between building walls (m)	24.000
3.	TX distance from left wall (m)	5.000
5.	TX height from street (m)	2.150
6.	RX distance from right wall (m)	5.000
8.	Minimum distance from TX to RX (m)	50.000
9.	Maximum distance from TX to RX (m)	950.000
10.	Step size in distance from TX to RX (m)	1.000
11.	RX height from street (m)	1.800
12.	Radio Frequency (GHz)	9.600
16.	TX ant. beamwidth (degrees)	30.000
17.	TX antenna gain (dB)	17.000
18.	TX ant. elevation angle (degrees)	0.000
22.	TX ant. azmuthal angle (left-neg., degrees)	0.000
26.	RX ant. beamwidth (degrees)	2.400
27.	RX antenna gain (dB)	38.000
28.	RX ant. elevation angle (degrees)	0.000
32.	RX ant. azmuthal angle (left-neg., degrees)	0.000
36.	Transmitter power (dBm)	18.500
38.	Loss for street reflection (dB)	1.000
39.	Loss for wall reflection (dB)	1.000
40.	Atmospheric Pressure (kPa)	83.000
41.	Relative Humidity (Percent)	50.000
42.	Temperature (Celsius)	20.000
43.	Are cross streets to be used (1=yes,0=no)	0.000
44.	Distance from TX to first cross street (m)	10.000
45.	Distance between cross streets (m)	76.000
46.	Width of cross street (m)	24.000
47.	Plot distribution: (0=no, 1=yes)	0.000
48.	Plot distribution separately: (0=no, 1=yes)	1.000
49.	Plot actual value: (0=no, 1=yes)	1.000
50.	Confidence interval (decimal)	0.900

Figure 18. The input parameter list for the data in Figure 17a. Only the frequency is different for Figures 17b and 17c.

Outputs produced to demonstrate the effect of antenna beamwidth are shown in Figure 19. In Figures 19a and 19b the transmitting antenna beamwidth is 30 degrees and the receiving antenna beamwidths are 2.4 and 30 degrees, respectively. The increased amplitude of the wall-reflected rays due to the increase in receiving antenna beamwidth results in much more rapid fading in Figure 19b than in Figure 19a. The ground-reflected component is essentially unchanged and the underlying interference pattern between the line-of-sight ray and the ground-reflected ray is nearly the same in both distance scans.

In the previous examples of model predictions, no cross streets were used, i.e., none of the rays were eliminated from the sum when computing the received signal level. The data in Figure 20 is presented to show the effect on the predictions when rays are eliminated which have specular reflection points located at the intersection of a cross street. Figure 20a shows the same range scan as Figure 19b. Figure 20b is the same range scan predicted by including cross streets in the model. Only slight differences are observed between Figures 20a (without cross streets) and 20b (with cross streets). This result is due to the non-symmetry of the terminal locations in the street. Contrasting results are seen in Figures 20c and 20d, where perfect street symmetry exists with the terminals located at the center of the street. Figure 20c now shows a much more regular fading pattern due to the symmetry. In effect, the unrealistic, perfect symmetry results in half of the rays having identical phase and amplitude to the other half. When cross streets are included for this case (Figure 20d), all wall-reflected rays are eliminated at some distances, giving very unrealistic results. As mentioned earlier, because reflection is determined by a surface area and not by a single point, it is much more realistic to assume that cross streets effect the amplitude and phase of a reflected ray but do not always eliminate it. The model predictions are therefore more realistic when building walls are modeled as continuous without cross streets.

5. COMPARISONS BETWEEN MEASUREMENTS AND THE MODEL

Measurements have been made in downtown Denver, Colorado (Violette et al., 1983) that can be compared to the range and azimuth scan outputs of the computer model. Measurements taken under a variety of conditions, e.g., with narrow and wide beamwidth antennas, have been selected to compare with the model predictions. In each case, the

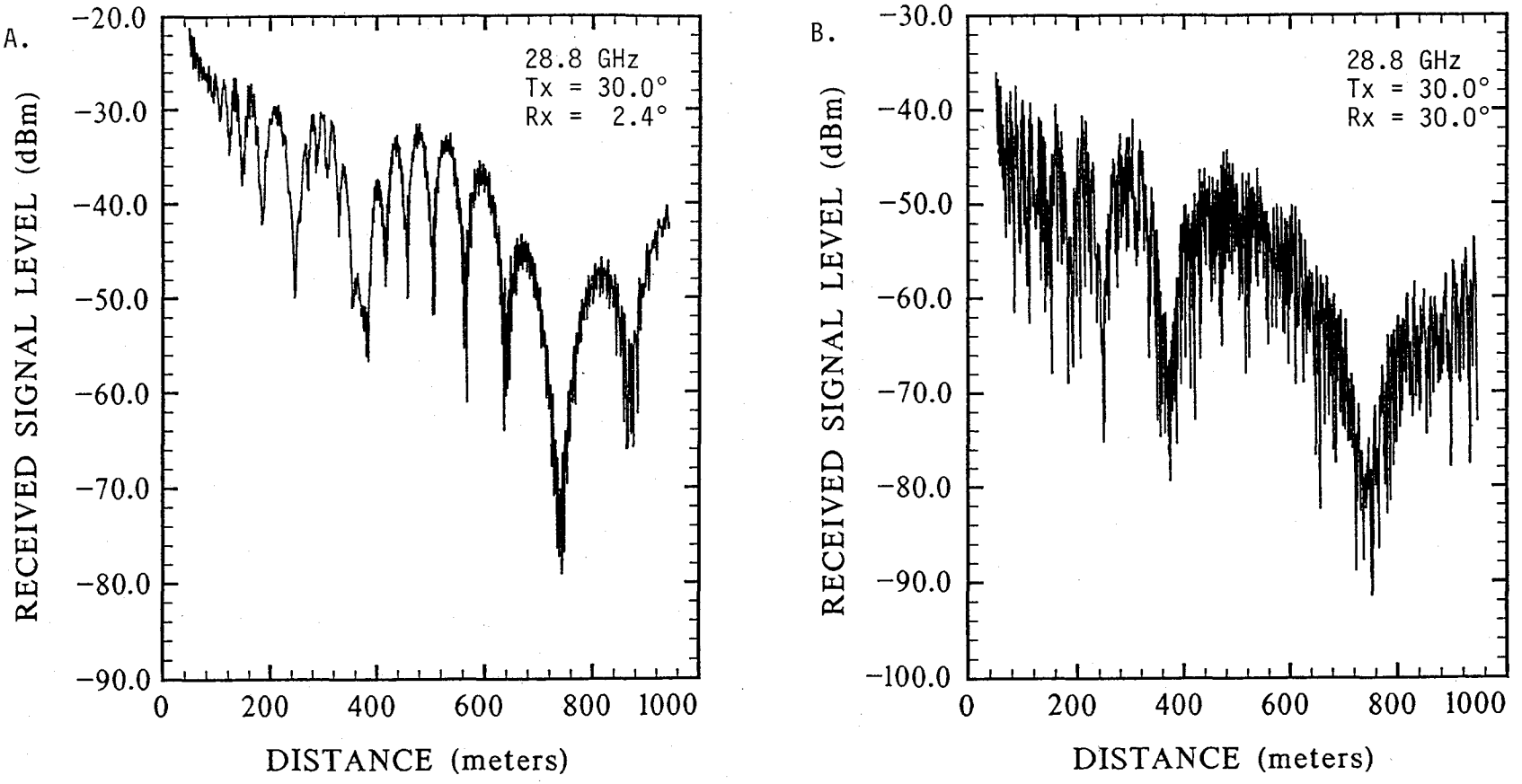

Figure 19. Range scans showing the effects of antenna beamwidth.

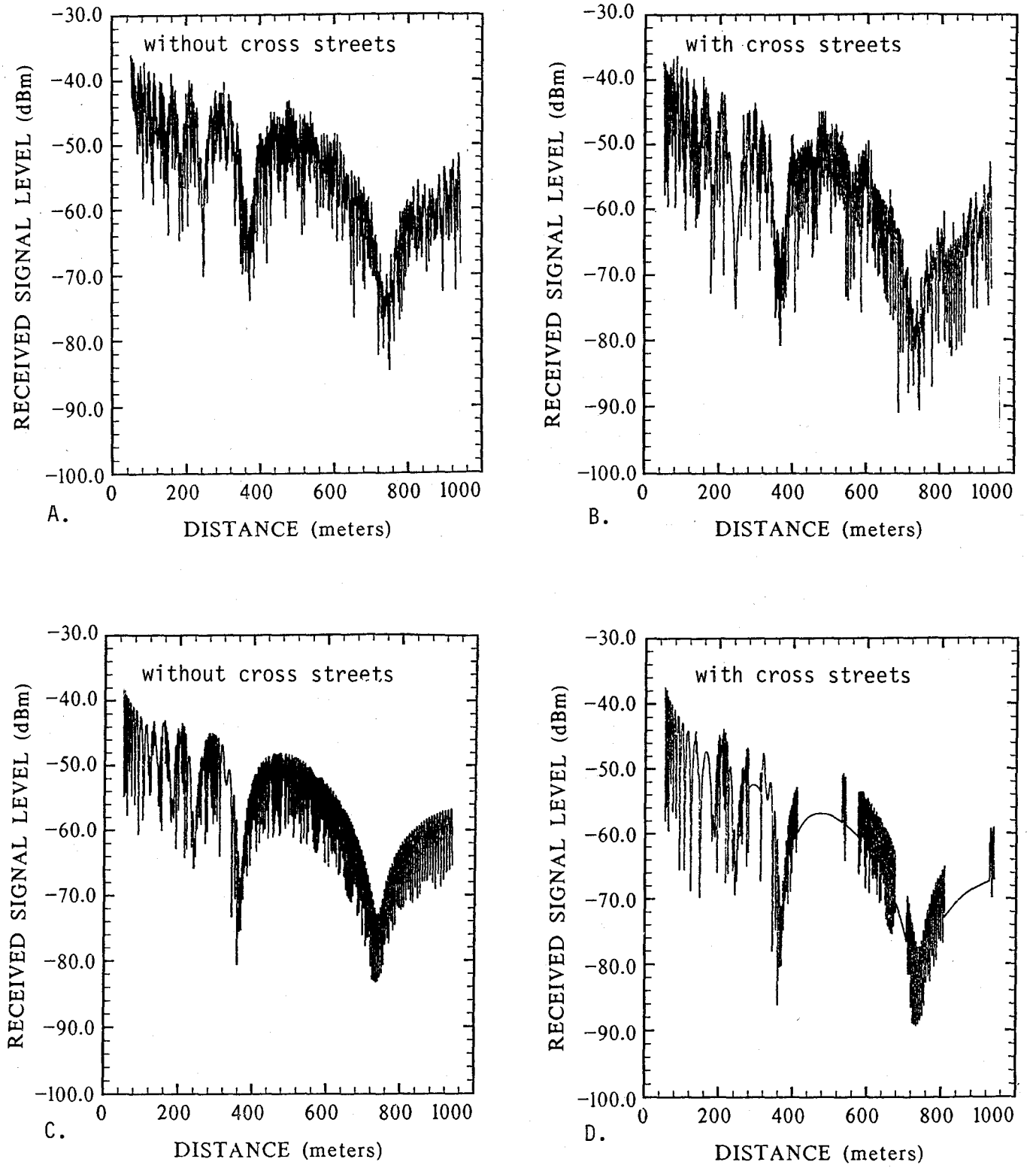

Figure 20. Range scans showing the effect of eliminating rays to account for cross streets. The symmetry of the terminals centered in the street increases the undesirable effect.

input parameters to the model (antenna beamwidths, street width, etc.) were set to match the measurement conditions.

The street- and wall-reflection-loss parameters were not known, but were set to values which resulted in the best match of the model outputs to the measured data. Based on the comparisons, realistic values of street-reflection loss are estimated to be between 0.5 and 3 dB. Average wall-reflection losses are probably between 0.5 and 6 dB per reflection.

The maximum number of wall reflections allowed in the computation of the model predictions was 3.

5.1 Range Scan Comparisons

Measurements of received signal level as a function of distance at 9.6, 28.8, and 57.6 GHz made on a nearly flat asphalt road are shown on the left side of Figure 21. The measurements were made in a rural area and there were no buildings along the road to cause reflections. The transmitting antennas had 10 degree beamwidths and were 2.15 meters above the road surface. The receiving antennas had beamwidths of 4.8, 1.2, and 1.2 degrees respectively at 9.6, 28.8, and 57.6 GHz and were 3.25 meters above the road surface. Range scans predicted by the model for each frequency are shown on the right side of Figure 21. The input parameter values used for these predictions are listed in Figure 22. To simulate an open road with no structures at the side of the road, the loss for wall reflections was set at 50 dB in the model.

In general, the measured and predicted data compare quite well at each frequency. The nulls in signal level occur at about the same distances and the signal levels are comparable. Some additional nulls occur in the measured data that are not in the predicted data, especially around 300 meters distance. The reason for the discrepancy between the measurements and the model predictions is not known. However, the road on which the measurements were made was not perfectly flat and uniform, and the motion of the vehicle on which the antennas were mounted might have caused some errors in antenna pointing. The signal roll-off at 28.8 Ghz and 57.6 GHz at short distances occurs because the transmitting and receiving antennas were mounted at different heights so that some misalignment occurred at short distances.

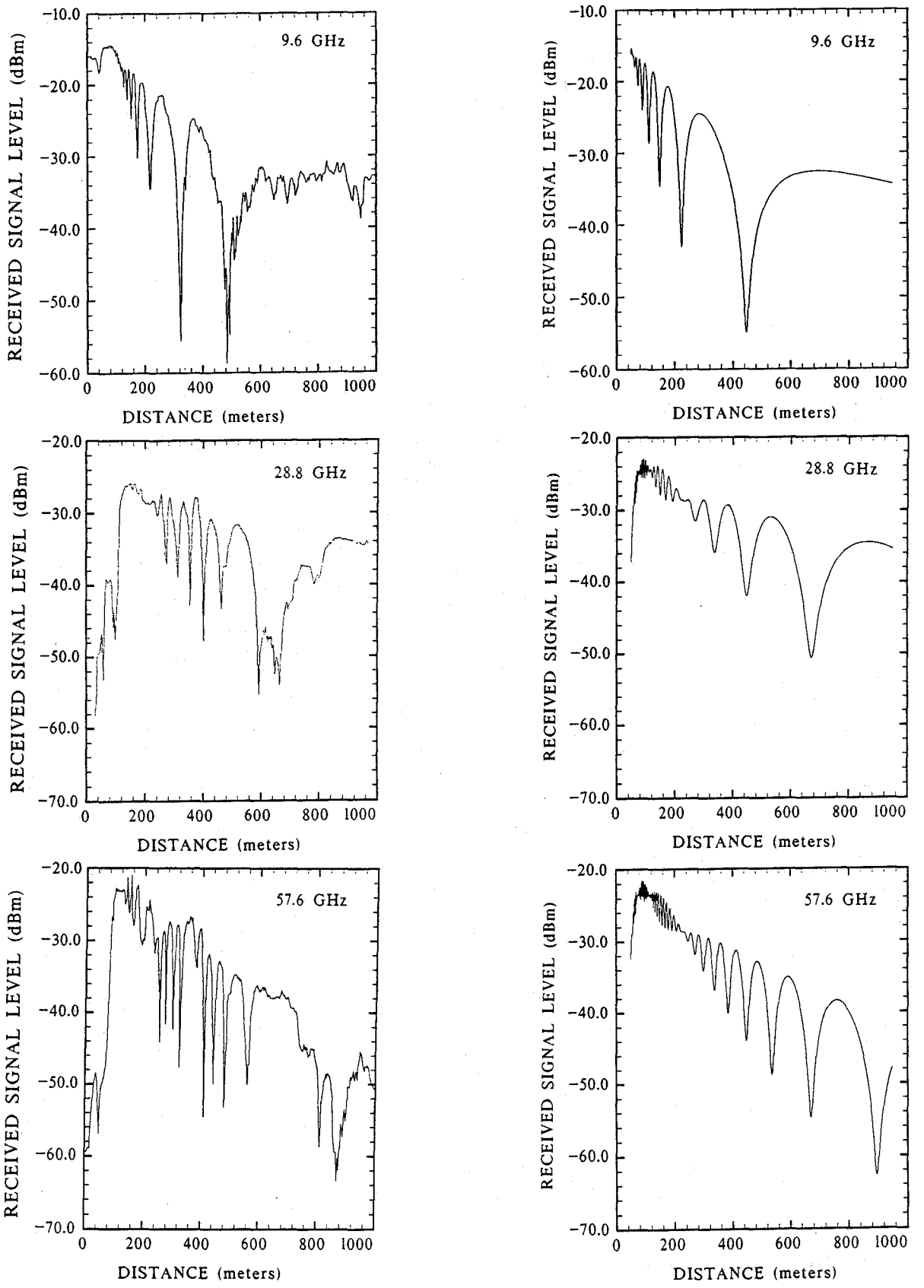

Figure 21. Range scans from the model and data measured in a rural area with transmitting and receiving antenna heights of 2.15 and 3.25 meters, respectively.

SUMMARY OF PARAMETERS

Index	Description	Value	Value	Value
1.	Maximum number of wall reflections (integer)	4.000	4.000	4.000
2.	Distance between building walls (m)	24.000	24.000	24.000
3.	TX distance from left wall (m)	12.000	12.000	12.000
5.	TX height from street (m)	2.150	2.150	2.150
6.	RX distance from right wall (m)	12.000	12.000	12.000
8.	Minimum distance from TX to RX (m)	50.000	50.000	50.000
9.	Maximum distance from TX to RX (m)	950.000	950.000	950.000
10.	Step size in distance from TX to RX (m)	1.000	1.000	1.000
11.	RX height from street (m)	3.250	3.250	3.250
12.	Radio Frequency (GHz)	9.600	28.800	57.600
16.	TX ant. beamwidth (degrees)	10.000	10.000	10.000
17.	TX antenna gain (dB)	25.000	25.000	25.000
18.	TX ant. elevation angle (degrees)	0.000	0.000	0.000
22.	TX ant. azmuthal angle (left-neg., degrees)	0.000	0.000	0.000
26.	RX ant. beamwidth (degrees)	4.800	1.200	1.200
27.	RX antenna gain (dB)	31.000	42.800	43.100
28.	RX ant. elevation angle (degrees)	0.000	0.000	0.000
32.	RX ant. azmuthal angle (left-neg., degrees)	0.000	0.000	0.000
36.	Transmitter power (dBm)	15.500	13.000	20.800
38.	Loss for street reflection (dB)	0.500	0.500	0.500
39.	Loss for wall reflection (dB)	50.000	50.000	50.000
40.	Atmospheric Pressure (kPa)	83.000	83.000	83.000
41.	Relative Humidity (Percent)	50.000	50.000	50.000
42.	Temperature (Celsius)	20.000	20.000	20.000
43.	Are cross streets to be used (1=yes,0=no)	0.000	0.000	0.000
44.	Distance from TX to first cross street (m)	10.000	10.000	10.000
45.	Distance between cross streets (m)	76.000	76.000	76.000
46.	Width of cross street (m)	24.000	24.000	24.000
47.	Plot distribution: (0=no, 1=yes)	0.000	0.000	0.000
48.	Plot distribution separately: (0=no, 1=yes)	1.000	1.000	1.000
49.	Plot actual value: (0=no, 1=yes)	1.000	1.000	1.000
50.	Confidence interval (decimal)	0.900	0.900	0.900

Figure 22. Input parameter values for the three frequencies in Figure 21.

In Figure 23, a second set of rural data is shown. The measurement conditions for this set were identical to the set in Figure 22, except that the receiving antennas were 1.00 meter above ground instead of 3.25 meters. This resulted in a much different signal level dependence on distance with fewer fades. The predicted data show a similar change in signal level dependence on distance and again agree well with the measurements in this set.

A set of measurement and model prediction data for an urban environment is shown in Figures 24, 25, and 26 for frequencies 9.6, 28.8, and 57.6 GHz, respectively. These data were taken along 17th Street in Denver. The operating conditions (antenna beamwidths and antenna heights) were similar to those used for Figure 22. The actual difference was the presence of buildings and cross streets in Denver as opposed to open fields for the rural measurements. The model input parameter values are listed in Figure 27. The street dimensions were set to match the physical size of 17th Street and the cross streets. The loss for wall reflections was set to 6 dB.

The top set of data in each figure was obtained with the antennas pointed parallel to the street. Good agreement can be seen between the measurements and predictions under this condition for all three frequencies. The middle and bottom set show results when the receiving antenna is off-pointed at 2 and 4 degrees, respectively, to the left (toward the far side of the street). The model predictions do not match the measured data as well under these off-pointing conditions. The predicted signal levels are sometimes too high and the effect of the cross streets is exaggerated. As is shown below, the measured antenna gain patterns were significantly different than the idealized patterns used in the model. The model antenna patterns had much higher side lobes which would be expected to result in higher signal levels under off-pointing conditions.

In Figure 28, a final set of range scan data at 28.8 GHz shows how measured and predicted data depend on antenna beamwidth. A 30 degree transmitting antenna was used for both measurements. The receiving antenna had a beamwidth of 2.4 degrees in the top set and a beamwidth of 30 degrees in the bottom set of the figure. The wider beamwidth receiving antenna resulted in much more rapid fading in both the measured and predicted data as would be expected because of the increased amplitude of the wall-reflected components of the signal.

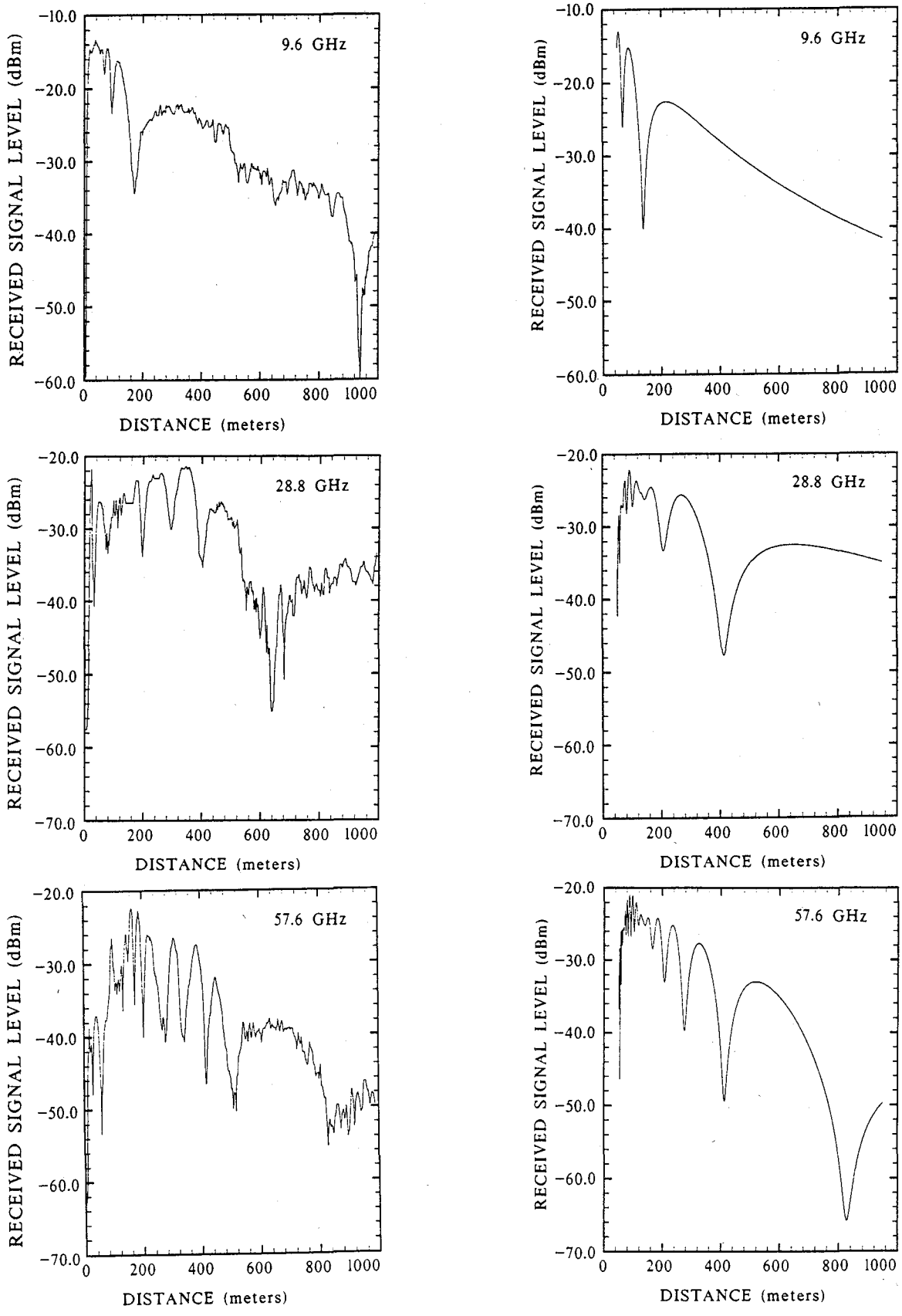

Figure 23. Range scans of model predicted data and measured data taken in a rural area with transmitting and receiving antenna heights of 2.15 and 1.00 meters.

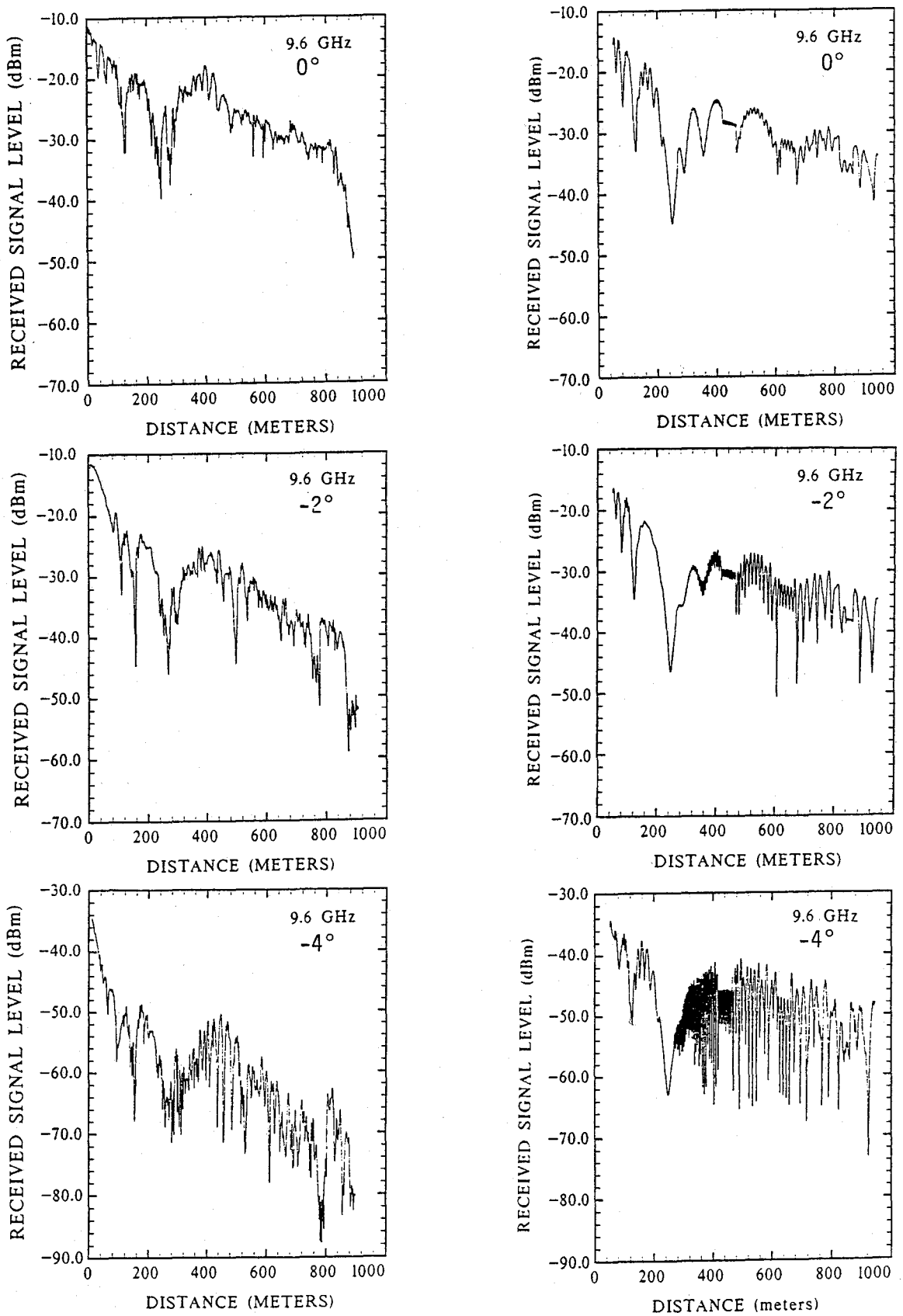

Figure 24. Range scans at 9.6 GHz of model predicted data (right side) and measured data (left side) taken in an urban area with transmitting and receiving antenna heights of 2.15 and 1.8 meters, respectively.

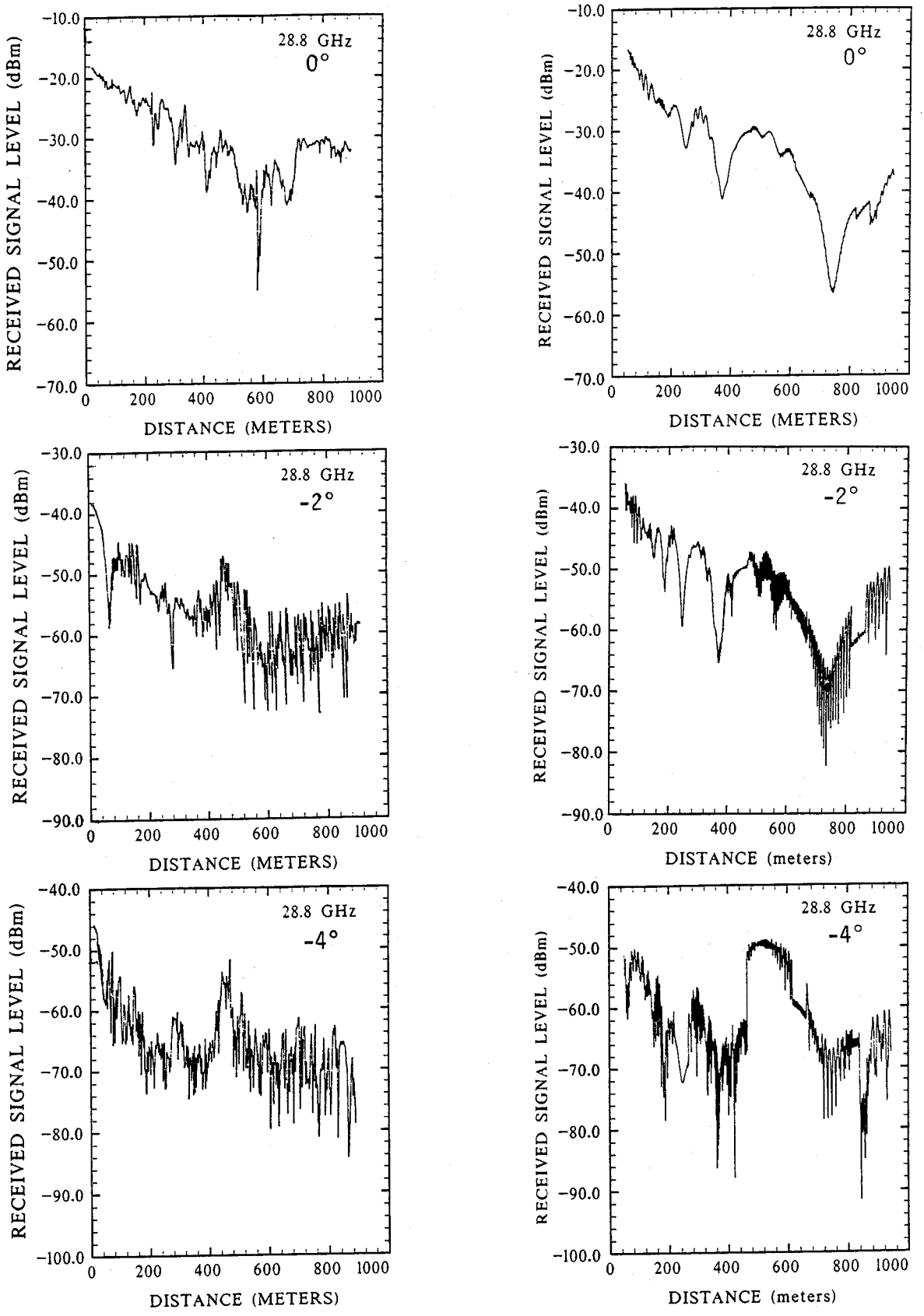

Figure 25. Range scans at 28.8 GHz of model predicted data (right side) and measured data (left side) taken in an urban area with transmitting and receiving antenna heights of 2.15 and 1.8 meters, respectively.

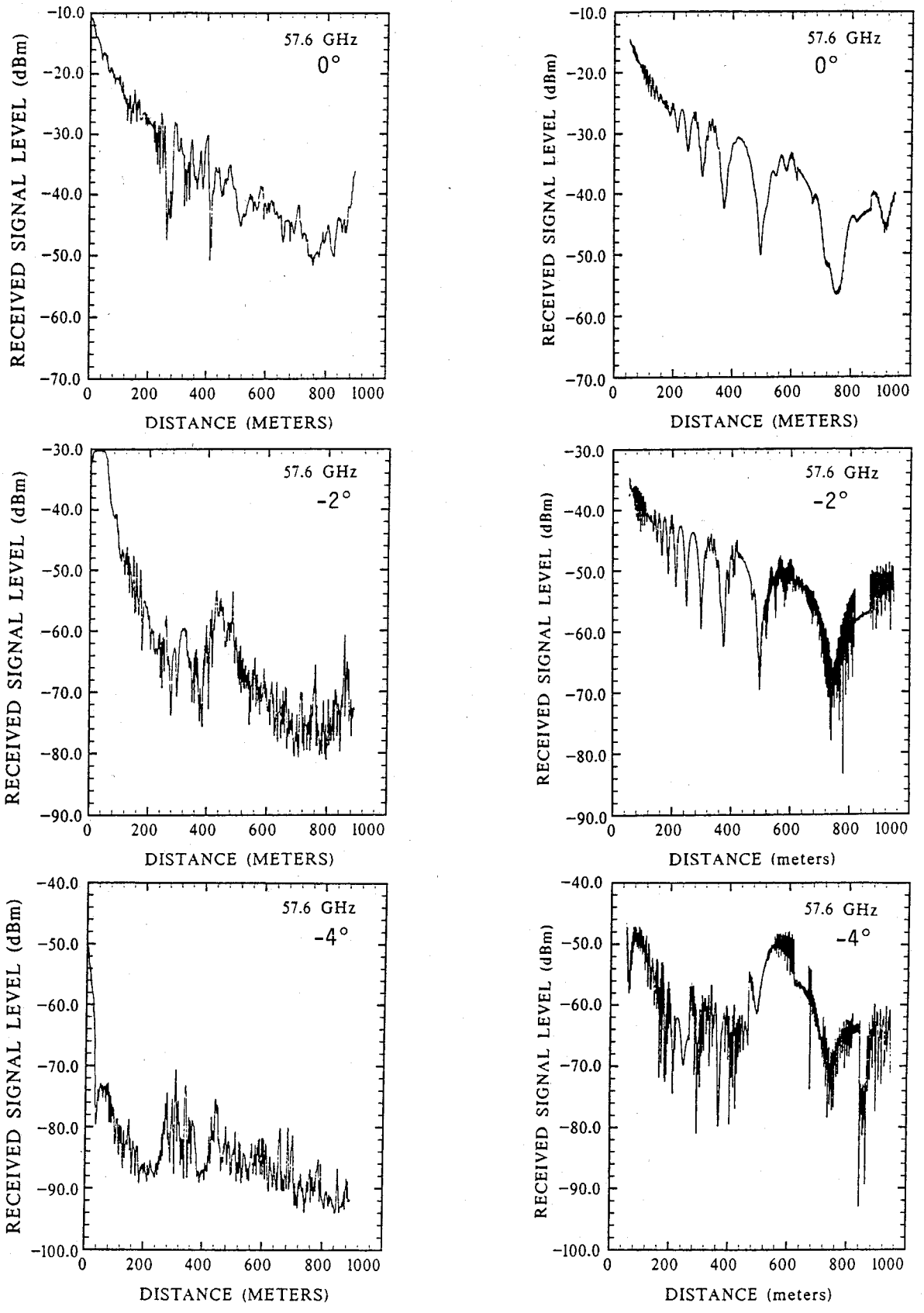

Figure 26. Range scans at 57.6 GHz of model predicted data (right side) and measured data (left side) taken in an urban area with transmitting and receiving antenna heights of 2.15 and 1.8 meters, respectively.

SUMMARY OF PARAMETERS

Index	Description	Value	Value	Value
1.	Maximum number of wall reflections (integer)	4.000	4.000	4.000
2.	Distance between building walls (m)	24.000	24.000	24.000
3.	TX distance from left wall (m)	5.000	5.000	5.000
5.	TX height from street (m)	2.150	2.150	2.150
6.	RX distance from right wall (m)	5.000	5.000	5.000
8.	Minimum distance from TX to RX (m)	50.000	50.000	50.000
9.	Maximum distance from TX to RX (m)	950.000	950.000	950.000
10.	Step size in distance from TX to RX (m)	1.000	1.000	1.000
11.	RX height from street (m)	1.800	1.800	1.800
12.	Radio Frequency (GHz)	9.600	9.600	9.600
16.	TX ant. beamwidth (degrees)	10.000	10.000	10.000
17.	TX antenna gain (dB)	25.000	25.000	25.000
18.	TX ant. elevation angle (degrees)	0.000	0.000	0.000
22.	TX ant. azmuthal angle (left-neg., degrees)	0.000	-2.000	-4.000
26.	RX ant. beamwidth (degrees)	4.800	4.800	4.800
27.	RX antenna gain (dB)	31.000	31.000	31.000
28.	RX ant. elevation angle (degrees)	0.000	0.000	0.000
32.	RX ant. azmuthal angle (left-neg., degrees)	0.000	0.000	0.000
36.	Transmitter power (dBm)	15.500	15.500	15.500
38.	Loss for street reflection (dB)	1.000	1.000	1.000
39.	Loss for wall reflection (dB)	6.000	6.000	6.000
40.	Atmospheric Pressure (kPa)	83.000	83.000	83.000
41.	Relative Humidity (Percent)	50.000	50.000	50.000
42.	Temperature (Celsius)	20.000	20.000	20.000
43.	Are cross streets to be used (1=yes,0=no)	1.000	1.000	1.000
44.	Distance from TX to first cross street (m)	10.000	10.000	10.000
45.	Distance between cross streets (m)	76.000	76.000	76.000
46.	Width of cross street (m)	24.000	24.000	24.000
47.	Plot distribution: (0=no, 1=yes)	0.000	0.000	0.000
48.	Plot distribution separately: (0=no, 1=yes)	1.000	1.000	1.000
49.	Plot actual value: (0=no, 1=yes)	1.000	1.000	1.000
50.	Confidence interval (decimal)	0.900	0.900	0.900

Figure 27. Input parameter values for the 9.6 GHz data in Figure 24 with 0, -2, and -4 degree pointing. Only the frequency was changed for Figures 25 and 26.

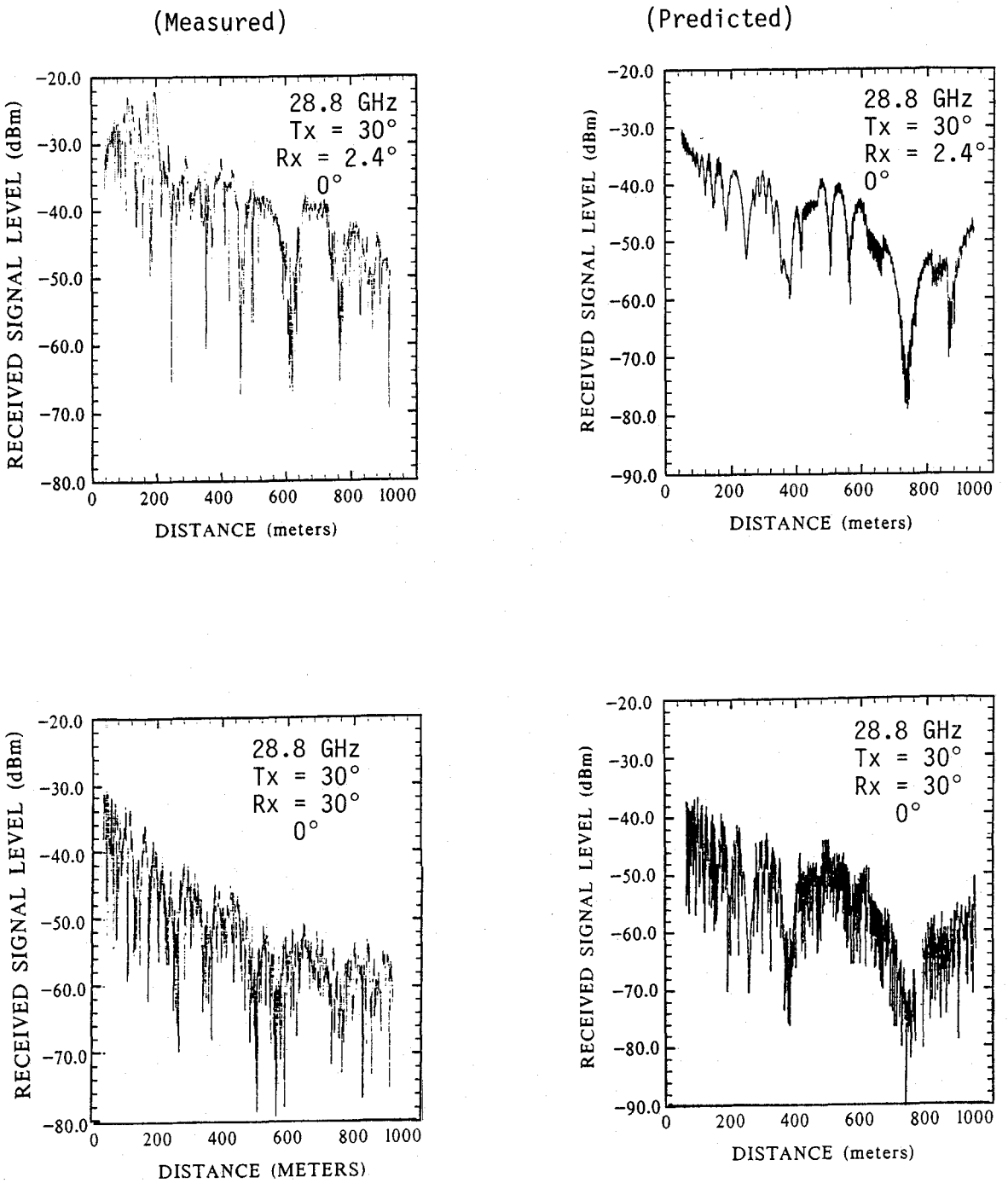

Figure 28. Range scans at 28.8 GHz, model (right side) and measured (left side), taken in an urban area. The receiving antenna beamwidth was 2.4 degrees in the upper pair and 30 degrees in the lower pair.

5.2 Azimuth Scan Comparisons

The data set in Figure 29 shows measured and predicted receiver azimuthal scan results at 9.6, 28.8, and 57.6 GHz for a path length of 485 meters. The model input parameter values used for the predicted data are given in Figure 30. These are the same parameter values as used for the on-line pointing data in Figures 23, 24, and 25. The measurements and model predictions show good agreement considering the model's idealized environment and antenna patterns. Even better agreement would be expected had the model antenna side lobes been more representative of the measurement antenna patterns. The measured and model antenna patterns are shown in Figure 31. Observe that the side lobes of the model antenna pattern are regular and much higher than the side lobes of the measurement antennas.

A comparison between the antenna patterns of the measurement antennas in Figure 31 and measured azimuthal scans in Figure 29 shows that there were signals arriving at wide azimuth angles. Signals at wide azimuth angles would have undoubtedly been seen in the model predictions from multiple wall reflections except that they were offset by the side lobes of the model antenna pattern. If antenna patterns which more closely matched the patterns of the measurement antennas had been used in the model, much better agreement would be expected between the measured and predicted azimuthal scans. However, on a real street, the reflection loss would sometimes be very high at one or more specular reflection points on a ray path, so that some reflected-ray paths would not result in measurable signals. Therefore, the predicted azimuthal scan would be expected to show some signals for which none appear in the measured data at the same azimuth angle.

6. SUMMARY

The telecommunications industry is anticipating the rapid development of personal mobile radio communications systems, such as the emerging personal communication networks (PCN). These networks are similar to today's cellular telephone technology. However, much smaller cell sizes are used and as a result the portable phone is much smaller (pocket size) and inexpensive.

The development of personal mobile radio communications is increasing the demand for already scarce radio spectrum. The millimeter-wave spectrum offers some unique

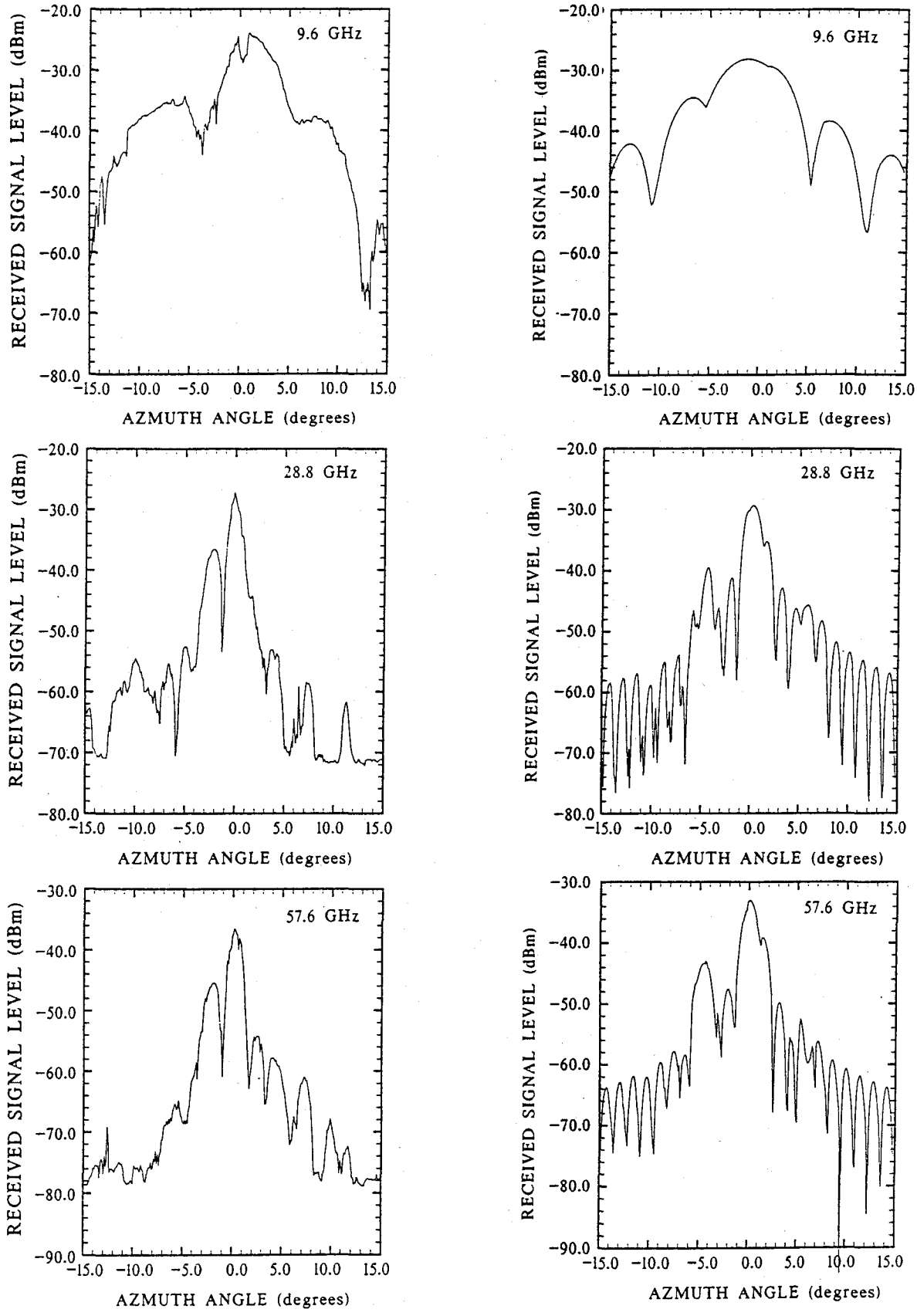

Figure 29. Azimuth scans at 9.6, 28.8, and 57.6 GHz. Model outputs are on the right and measurements made on a 485 meter path are on the left.

SUMMARY OF PARAMETERS

Index	Description	Value	Value	Value
1.	Maximum number of wall reflections (integer)	4.000	4.000	4.000
2.	Distance between building walls (m)	24.000	24.000	24.000
3.	TX distance from left wall (m)	5.000	5.000	5.000
5.	TX height from street (m)	2.150	2.150	2.150
6.	RX distance from right wall (m)	5.000	5.000	5.000
7.	RX distance from TX (m)	485.000	485.000	485.000
11.	RX height from street (m)	1.800	1.800	1.800
12.	Radio Frequency (GHz)	9.600	28.800	57.600
16.	TX ant. beamwidth (degrees)	10.000	10.000	10.000
17.	TX antenna gain (dB)	25.000	25.000	25.000
22.	TX ant. azmuthal angle (left-neg., degrees)	0.000	0.000	0.000
26.	RX ant. beamwidth (degrees)	4.800	1.200	1.200
27.	RX antenna gain (dB)	31.000	42.800	43.100
28.	RX ant. elevation angle (degrees)	0.000	0.000	0.000
29.	Minimum RX elevation angle (degrees)	-5.000	-5.000	-5.000
30.	Maximum RX elevation angle (degrees)	5.000	5.000	5.000
31.	Step size in RX elevation angle (degrees)	0.010	0.010	0.010
32.	RX ant. azmuthal angle (left-neg., degrees)	0.000	0.000	0.000
33.	Minimum RX azmuthal angle (degrees)	-15.000	-15.000	-15.000
34.	Maximum RX azmuthal angle (degrees)	15.000	15.000	15.000
35.	Step size in RX azmuthal angle (degrees)	0.100	0.100	0.100
36.	Transmitter power (dBm)	15.500	13.000	20.800
37.	Receiver noise figure (dB)	6.000	6.000	6.000
38.	Loss for street reflection (dB)	1.000	1.000	1.000
39.	Loss for wall reflection (dB)	6.000	6.000	6.000
40.	Atmospheric Pressure (kPa)	83.000	83.000	83.000
41.	Relative Humidity (Percent)	50.000	50.000	50.000
42.	Temperature (Celsius)	20.000	20.000	20.000
43.	Are cross streets to be used (1=yes,0=no)	1.000	1.000	1.000
44.	Distance from TX to first cross street (m)	10.000	10.000	10.000
45.	Distance between cross streets (m)	76.000	76.000	76.000
46.	Width of cross street (m)	24.000	24.000	24.000
47.	Plot distribution: (0=no, 1=yes)	0.000	0.000	0.000
48.	Plot distribution separately: (0=no, 1=yes)	1.000	1.000	1.000
49.	Plot actual value: (0=no, 1=yes)	1.000	1.000	1.000
50.	Confidence interval (decimal)	0.900	0.900	0.900

Figure 30. Model input parameter values for the three frequencies in Figure 29.

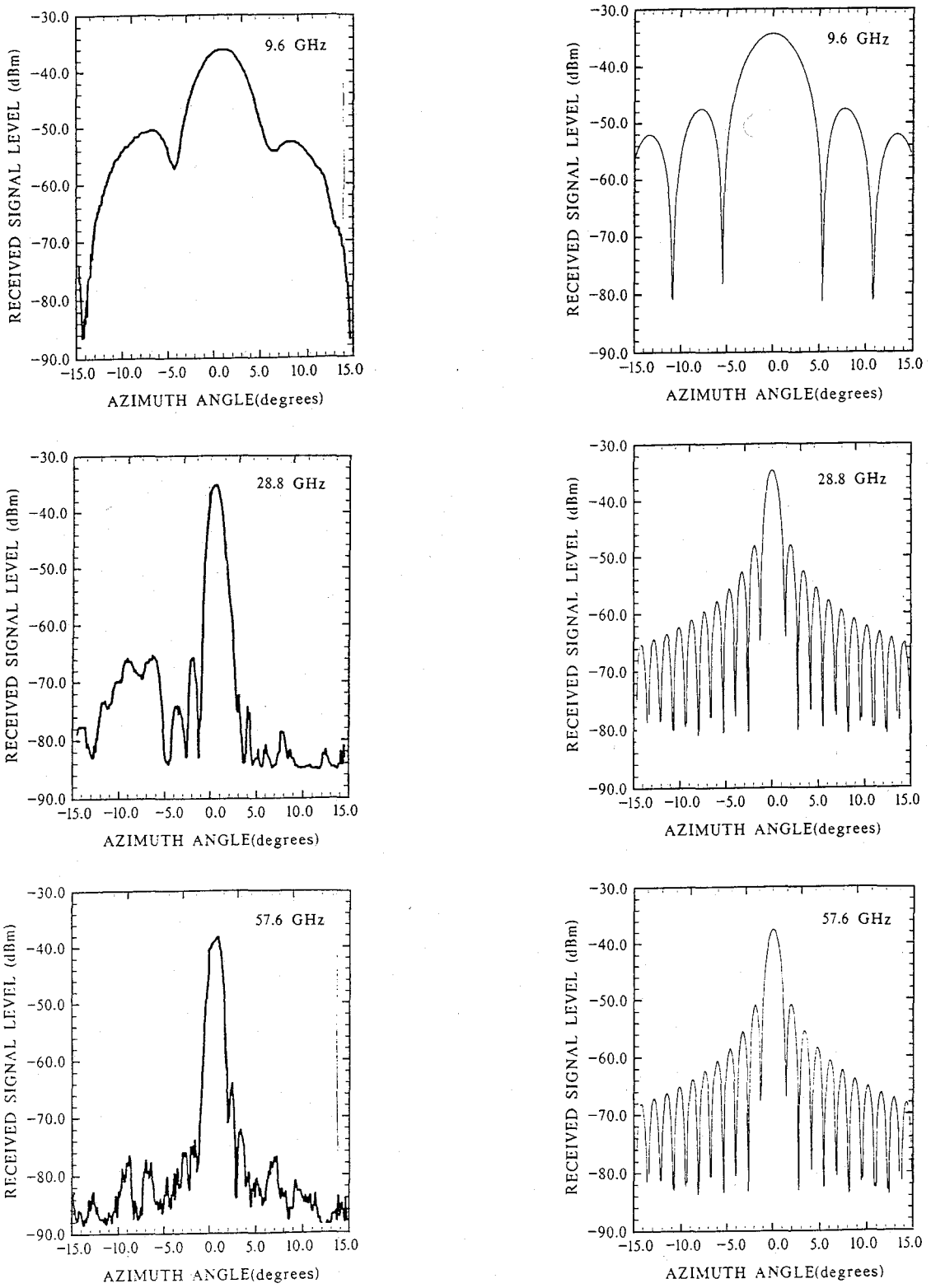

Figure 31. Azimuth scans showing the antenna patterns of the antennas used to make the measurements (left side) and the patterns used in the model (right side).

advantages for PCN applications. The primary advantage is spectrum availability, particularly for the wideband digital services expected in the future. Other advantages are the small size and integrated circuit manufacturing technology that are possible for millimeter-wave devices. Finally, the absorption of millimeter waves by the atmosphere decreases the likelihood of interference and increases the opportunities for frequency reuse.

In order to take advantage of millimeter waves for PCN, their propagation on short paths in various environments needs to be adequately understood. Some measurements of millimeter-wave propagation in urban and suburban environments have been reported (Violette et al., 1883, 1985, 1988a, 1988b). The measurements of particular interest here were made on line-of-sight paths within the first few meters above street level in an urban environment. These measurements indicated that most of the energy arriving at the receiver came either directly by line of sight, or was reflected from buildings up to several times. Scattered and diffracted energy did not seem to contribute significantly for line-of-sight paths.

A model for millimeter-wave propagation on such paths in urban environments was developed based on the geometrical optics theory to account for the direct and reflected modes of propagation. By assuming that the reflected rays have random phase, a statistical model of received signal amplitude was derived for an ensemble of urban streets. The resulting distribution of signal amplitude was Nakagami-Rice where the line-of-sight and street-reflected rays were assumed to compose a known signal component.

The Nakagami-Rice distribution was approximated by the Weibull distribution. A method for computing a satisfactory value of the single parameter (slope) of the Weibull distribution from the single parameter (ratio of power in constant and random components) of the Nakagami-Rice distribution was derived.

Comparisons were made between the geometrical optics model predictions and measurements showing received signal level as a function of separation distance between the transmitter and receiver and azimuth pointing angle of the receiving antenna. The measurements generally validated the model.

The few discrepancies between the model predictions and the measured data could be attributed to two sources. One was the way cross streets were treated in the model. Often a ray path would have a reflection point at an intersection of a cross street where

there was no building from which to reflect. If the ray was then eliminated and the path treated as invalid, the received signal level sometimes showed discontinuities as a function of distance which were unrealistic and were never seen in measurements. If the ray was treated normally, realistic predictions resulted. This is thought to be attributable to the fact that reflection is a surface activity and not a point activity. A gap in the buildings along a street caused by a cross street would then be expected to effect the amplitude and phase of a reflected ray but not totally eliminate it. This is especially true at shallow reflection angles for which the Fresnel zones of reflection are large.

The second cause of discrepancies between predictions and measured data was the difference between the antenna patterns assumed in the model and those of the antennas used to make the measurements. The higher side-lobe levels of the model antenna patterns caused errors when the antennas were pointed off the line of sight, toward the buildings on the side of the street. They also hid weak reflections from the walls in the predictions of signal level as a function of antenna azimuth angle pointing.

With correction for the above weaknesses in the model, it should be effective when used to simulate signals to test various PCN scenarios or system designs and to give a priori statistics of received signal level on line-of-sight paths in urban environments.

Earlier reported results (Violette et al., 1983) show that the geometrical theory of diffraction could be used to model millimeter-wave diffraction around buildings. A complete model of millimeter-wave propagation for arbitrary paths in urban environments can be developed by combining the geometrical optics model for line-of-sight paths with the geometrical theory of diffraction model for non-line-of-sight paths.

7. REFERENCES

Beckman, P., and A. Spizzichino (1963), "The Scattering of Electromagnetic Waves from Rough Surfaces," Macmillan Co., NY.

Hufford, G.A., and D.R. Ebaugh, Jr. (1985), A study of interference fields in a ducting environment, NTIA Report 85-177, June, 50 pp. (NTIS order no. PB 85- 242998).

Liebe, H.J. (1985), An updated model for millimeter wave propagation in moist air, Radio Science, 20, No. 5, Sep - Oct, pp. 1069-1089.

Nakagami, M. (1940), Study on the resultant amplitude of many vibrations whose phase and amplitudes are random, Nippon Elect. Comm. Eng., 22, October, pp. 69-92.

Rice, P.L., A.G. Longley, K.A. Norton, and A.P. Barsis (1967), Transmission loss predictions for tropospheric communications circuits, NBS Technical Note 101 (revised).

Rice, S.O. (1945), Mathematical analysis of random noise, Bell System Tech. J., 33, Jan, pp. 417-504.

Violette, E.J., R.H. Espeland, K.C. Allen, and F. Schwering (1983), Urban millimeter wave propagation studies, Research and Development Technical Report, CECOM-83-3, U.S. Army Communications-Electronics Command, Fort Monmouth, NJ 07703, Apr.

Violette, E.J., R.H. Espeland, G.R. Hand (1985), Millimeter-wave urban and suburban propagation measurements using narrow and wide bandwidth channel probes, NTIA Report 85-184, Nov, 95 pp. (NTIS order no. PB 86-147741).

Violette, E.J., R.H. Espeland, R.O. DeBolt, and F. Schwering (1988a), Millimeter-wave propagation at street level in an urban environment, IEEE Trans. Geosci. and Remote Sensing, 26, No. 3, May, pp. 368-380.

Violette, E.J., R.H. Espeland, and K.C. Allen (1988b), Millimeter-wave propagation characteristics and channel performance for urban-suburban environments, NTIA Report 88-239, Dec, 178 pp. (NTIS order no. PB 89-180251/AS).

Weibull, W. (1951), A statistical distribution function of wide applicability, J. Appl. Mech. 18, pp. 203-297.

APPENDIX

The FORTRAN subroutines for computing the geometry of the ray paths are listed on the following pages.

```
c-------------------------------------------------------------
      SUBROUTINE Raypaths
c**********************************************************************
c     This subroutine computes the ray paths for the given geometry.
c     The TX location must be given as XT,YT=0,ZT and the receiver
c     location is given by XR,YR,ZR.  The street width is given
c     by WIDTH. These values are passed through the common labeled
c     Urban1.
c
c     The output is passed through the common labeled Urban5.
c     The following scheme is used:
c     Index1   =      1 for nonground reflected rays, 2 for ground
c                     reflected rays
c     Index2   =      index of ray from 1 to 2*MAXR+1 for the rays
c                     with N from -MAXR to MAXR
c     Index3   =      index of reflection point for each ray, from 1 to
c                     MAXR, with MAXR+1 used for ground reflection point
c     PATHLENGTH(Index1,Index2)      =      double precision path length
c     ANGLE(Index1,Index2,1)     =      azimuth of ray at tx, pos=right,neg=left
c       " ( "  , "  ,2)       =      elevation angle of ray at tx
c       " ( "  , "  ,3)       =      azimuth of ray at rx, pos=right,neg=left
c       " ( "  , "  ,4)       =      elevation angle of ray at rx
c       " ( "  , "  ,5)       =      angle of reflection from normal to walls
c       " ( "  , "  ,6)       =       "   "   "      from normal to
c                                    ground
c     REFLECTPTS(Index1,Index2,Index3,1)     =      X co-ordinate, reflection pt
c         " ( " , " , " ,2)    =      Y     "   ,      "    "
c         " ( " , " , " ,3)    =      Z     "   ,      "    "
c
c     Other variables:
c     M        =      image index, 1= above ground, -1= below ground
c     N        =      image index, 0= real location, neg=left, pos=right
c     MAXR     =      maximum number of wall reflections a ray is allowed
c     CROSS    =      parameter 43, 0=no cross streets, 1=yes
c**********************************************************************
```

```
      Common /Urban1/ MAXR,XT,YT,ZT,XR,YR,ZR,XI,YI,ZI,WIDTH
      Common /Urban5/ PATHLENGTH(2,21),ANGLE(2,21,6),
     +REFLECTPTS(2,21,11,3),OUT(2,21)
      Common /Urban7/ CROSS
      Integer CROSS
      Real*8 PATHLENGTH
      If (CROSS .ne. 0) Call CSL
      Do 100 M=-1,1,2
      Do 200 N=-MAXR,MAXR
      Call Image (M,N)
      Call DSTs
      Call Angles (M,N)
      Call Locations (M,N)
      Call CS (M,N)
      Call Packinfo (M,N)
200   Continue
100   Continue
      Return
      End


      SUBROUTINE Image (M,N)
c**********************************************************************
c     This subroutine computes the location of the M,N image of the
c     receiver.
c     XR        = X co-ordinate of real receiver, dist left from wall
c     YR        = Y     "      "   "    "    , dist from tx
c     ZR        = Z     "      "   "    "    , height above ground
c     M         = image index, 1= above ground, -1= below ground
c     N         =    "   " , 0= real location, neg=left, pos=right
c     WIDTH     = width of street
c     XI        = X co-ordinate of M,N image
c     YI        = Y     "      "   "    "
c     ZI        = Z     "      "   "    "
c**********************************************************************
      Common /Urban1/ MAXR,XT,YT,ZT,XR,YR,ZR,XI,YI,ZI,WIDTH
c
      XI=WIDTH*(N+(1-(-1)**N)/2)+XR*(-1)**N
      YI=YR
      ZI=M*ZR
      Return
      End
```

```
      SUBROUTINE DSTs
c*****************************************************************
c     This subroutine computes the distances associated with each
c     path.
c     XT        = X co-ordinate of TX, dist left from wall
c     YT        = Y     "      "   ", reference = 0
c     ZT        = Z     "      "   ", height above ground
c     XI        = X co-ordinate of M,N RX image
c     YI        = Y     "      "   "  "   "
c     ZI        = Z     "      "   "  "   "
c     PATHDX    = change in X co-ordinate from TX to M,N RX image
c     PATHDY    =    "   "  Y     "        "    "  "   "   "
c     PATHDZ    =    "   "  Z     "        "    "  "   "   "
c     HDIST     = horizontal distance between TX and M,N RX image
c     TDIST     = true distance between TX and M,N RX image
c*****************************************************************
      Common /Urban1/ MAXR,XT,YT,ZT,XR,YR,ZR,XI,YI,ZI,WIDTH
      Common /Urban2/ PATHDX,PATHDY,PATHDZ,HDIST,TDIST
      Real*8 HDIST,TDIST
c
      PATHDX=XI-XT
      PATHDY=YI-YT
      PATHDZ=ZI-ZT
      HDIST=SQRT(PATHDX**2+PATHDY**2)
      TDIST=SQRT(PATHDX**2+PATHDY**2+PATHDZ**2)
      Return
      End
```

```
      SUBROUTINE Angles (M,N)
c*****************************************************************
c     This subroutine computes the angles below for the M,N image.
c     AZMUTHTX  = azmuthal angle from TX to M,N RX image
c     ELEVATTX  = elevation angle from TX to M,N RX image
c     AZMUTHRX  = azmuthal angle from M,N RX image to TX
c     ELEVATRX  = elevation angle from M,N RX image to TX
c     GROUNDANG = angle of ground reflection with respect to grazing
c     WALLANG   = angle of wall reflection with respect to grazing
c     Other variable are:
c     M         = image index, 1= above ground, -1= below ground
c     N         =   "     " , 0= real location, neg=left, pos=right
c     PATHDX    = change in X co-ordinate from TX to M,N RX image
c     PATHDY    =    "  "  Y     "        "   "  "   "   "   "
c     PATHDZ    =    "  "  Z     "        "   "  "   "   "   "
c     HDIST     = horizontal distance between TX and M,N RX image
c*****************************************************************
      Common /Urban2/ PATHDX,PATHDY,PATHDZ,HDIST,TDIST
      Common /Urban3/ AZMUTHTX,AZMUTHRX,ELEVATTX,ELEVATRX,
     +GROUNDANG,WALLANG
      Real*8 TDIST,HDIST
c
c     Angles in radians
      AZMUTHTX=atan(PATHDX/PATHDY)
      AZMUTHRX=AZMUTHTX*(-1)**N
      ELEVATTX=atan(PATHDZ/HDIST)
      ELEVATRX=-M*ELEVATTX
      GROUNDANG=trueangl(PATHDX,PATHDY,PATHDZ,0.,0.,1.)
      WALLANG=trueangl(PATHDX,PATHDY,PATHDZ,1.,0.,0.)
c     Convert to grazing angles
      GROUNDANG=abs(1.5708-GROUNDANG)
      WALLANG=abs(1.5708-WALLANG)
      Return
      End
```

```
      SUBROUTINE Locations (M,N)
c*****************************************************************
c     This subroutine computes the locations of the points of
c     reflection for each ray path.  The locations are stored in the
c     array REFLECTIONS(INDEX1,INDEX2) where:
c          INDEX1=1 to abs(N) and is the wall reflection number
c                 =abs(N)+1 for the ground reflection
c          INDEX2=1 for X co-ordinate of reflection location
c                =2  "  Y     "     "     "        "
c                =3  "  Z     "     "     "        "
c     Other variable are:
c     M         = image index, 1= above ground, -1= below ground
c     N         =    "    "  , 0= real location, neg=left, pos=right
c     WIDTH     = width of street
c     XT        = X co-ordinate of TX, dist left from wall
c     YT        = Y     "     "  ", reference = 0
c     ZT        = Z     "     "  ", height above ground
c     PATHDX    = change in X co-ordinate from TX to M,N RX image
c     PATHDY    =    "  "  Y     "        "  "  "  "  "  "
c     PATHDZ    =    "  "  Z     "        "  "  "  "  "  "
c*****************************************************************
      Common /Urban1/ MAXR,XT,YT,ZT,XR,YR,ZR,XI,YI,ZI,WIDTH
      Common /Urban2/ PATHDX,PATHDY,PATHDZ,HDIST,TDIST
      Common /Urban4/ REFLECTIONS(11,3)
      Real*8 HDIST,TDIST
c
      If (N.eq.0) Then
c         This is an image RX with no wall reflections.
      Else
c         This is an image RX with wall reflections.
          Do 100 I=1,abs(N)
          If (N.gt.0) Then
c         N is positive, image walls to right
              XREF=I*WIDTH
              REFLECTIONS(I,1)=WIDTH*mod(I,2)
          Else
c         N is negative, image walls to left
              XREF=(1-I)*WIDTH
              REFLECTIONS(I,1)=WIDTH*mod(I+1,2)
          End if
          REFLECTIONS(I,2)=YT+(XREF-XT)*PATHDY/PATHDX
          REFLECTIONS(I,3)=abs(ZT+(XREF-XT)*PATHDZ/PATHDX)
100        Continue
      Endif
```

```
c
      If (M.eq.1) Then
c        This is an above ground image, no ground reflection
      Else
c        This is a below ground image, there is a ground reflection
         I=abs(N)+1
         XREF=XT-ZT*PATHDX/PATHDZ
         IXREF=Int(XREF/WIDTH)
         If (N.lt.0) IXREF=IXREF-1
         If (Mod(IXREF,2).eq.0) Then
c        even-nonreversed image
            REFLECTIONS(I,1)=XREF-IXREF*WIDTH
         Else
c        odd-reversed image
            REFLECTIONS(I,1)=WIDTH-(XREF-IXREF*WIDTH)
         End if
         REFLECTIONS(I,2)=YT-ZT*PATHDY/PATHDZ
         REFLECTIONS(I,3)=0
      Endif
      Return
      End
```

```
      SUBROUTINE CS (M,N)
c*****************************************************************
c     This subroutine determines if any of the rays strike a cross
c     street. Rays that strike a cross street are marked with a flag
c     that is stored in the array OUT (INDEX1,N). If OUT(INDEX1,N)=0, that
c     ray (M,N) may be removed from the Addrays subroutine.
c     The array REFLECTIONS (INDEX1,INDEX2) contains the location
c      of the points of reflection where:
c         INDEX1=1 to abs(N) and is the wall reflection number
c         INDEX2= the Y co-ordinate of the reflection point
c     Other variables are:
c     M          = image index, 1= above ground, -1= below ground
c     N          =  "     " , 0= real location, neg=left, pos=right
c     DNO,DN     = the ratio of the distance between the receiver and
c                 transmitter to the length of the block plus the
c                 width of the cross street
c     TXPOS      = the Y distance between the transmitter and the
c                 first cross street
c     BLOCK      = the distance between cross streets
c     LANE=       the width of the cross street
c     YR         =the Y co-ordinate of the receiver
c     LB(I)      = the Y co-ordinate of the beginning of a cross street
c     LE(I)      = the Y co-ordinate of the end of the cross street
c     CSN        = the number of cross streets
C     CROSS      = parameter 43, 0=no cross streets, 1=yes
c*****************************************************************
```

```
      Common /Urban5/ PATHLENGTH(2,21),ANGLE(2,21,6),REFLECTPTS(2,21,11,3),
     +OUT(2,21)
      Common /Urban1/ MAXR,XT,YT,ZT,XR,YR,ZR,XI,YI,ZI,WIDTH
      Common /Urban4/ REFLECTIONS(11,3)
      Common /Urban6/ BLOCK,LANE,TXPOS,DNO,LB(20),LE(20),L1,L2,DN
      Common /Urban7/ CROSS
      Real*8 LANE,BLOCK,TXPOS,L1,L2,DN,PATHLENGTH
      Integer DNO,CSN,CROSS
c
      If (CROSS .eq. 0) Goto 21
      If (N .eq. 0) Goto 21
      If (YR .le. TXPOS) Goto 21
c     Determines the number of cross streets
      CSN=1
      If (DNO .eq. 0) Goto 22
      Do 100 i=1,DNO
         CSN=I
         If (DN .gt. I) CSN=I+1
100   Continue
22    INDEX1=Indexone (M)
      INDEX2=Indextwo (MAXR,N)
C     WRITE (1,*) OUT (INDEX1,INDEX2)
      OUT (INDEX1,INDEX2)=0
      Do 200 I=1,Abs(N)
      Do 20 J=1,CSN
         If (REFLECTIONS(I,2) .le. LB(J)) Goto 20
         If (REFLECTIONS(I,2) .lt. LE(J)) OUT(INDEX1,INDEX2)=1
20    Continue
200   Continue
      Goto 21
21    Return
      End
```

```
      SUBROUTINE CSL
c*****************************************************************
c     This subroutine determines the Y co-ordinate range occupied
c     by each cross street. The values of the Y co-ordinates of the
c     beginning of a street are stored in the array LB(I). The values
c     of the Y co-ordinates of the end of streets are stored in the
c     array LE(I).
c     Other variables are:
c     YR          = Y co-ordinate of the receiver
c     DNO,DN       = the ratio of the distance between the receiver
c                    and the beginning of the first cross street to
c                    the sum of the block length and the street width
c     BLOCK       = the length of the block
c     LANE        = the width of the cross street
c     TXPOS       = the distance between the Tx and the first street
c*****************************************************************
      Common /Urban1/ MAXR,XT,YT,ZT,XR,YR,ZR,XI,YI,ZI,WIDTH
      Common/Urban6/ BLOCK,LANE,TXPOS,DNO,LB(20),LE(20),L1,L2,DN
      Common/Urban5/ PATHLENGTH(2,21),ANGLE(2,21,6),
     +REFLECTPTS(2,21,11,3),OUT(2,21)
      Integer DNO,DN1
      Real*8 LANE,BLOCK,TXPOS,L1,L2,DN
c
c     Clear OUT array
      Do 200 i=1,2
      Do 300 j=1,21
        OUT(I,J)=0
300   Continue
200   Continue
      If (YR .le. TXPOS) Goto 100
c     Read in parameter values
      LB(1)=TXPOS
      LE(1)=TXPOS+LANE
      L1=YR-TXPOS
      L2=BLOCK+LANE
      DNO=nint(L1/L2)
      DN=L1/L2
```

```
      If (DNO .le. 2) Then
          Goto 12
c     If two or more full blocks
      Else
          Do 400 I=2,DNO
          LB(I)=LE(I-1)+BLOCK
          LE(I)=LB(I)+LANE
          If ((LB(I)+LANE) .gt. YR) LE(I)=YR
          If (DN .gt. DNO) Then
              DN1=DNO+1
              LB(DN1)=LE(DNO)+BLOCK
              LE(DN1)=LB(DN1)+LANE
              If ((LB(DN1)+LANE) .gt. YR) LE(DN1)=YR
              Endif
400           Continue
      Endif
      Goto 100
 12   Continue
      If (L1 .lt. LANE) Then
          LE(1)=YR
          Goto 100
      Else if (DN .lt. 2) Then
          LB(2)=LE(1)+BLOCK
          LE(2)=LB(2)+LANE
          Goto 100
      Endif
c     If only 1 full block exists with 2 cross streets
      If (DN .lt. 2.5) Then
          Do 500 i=2,3
          LB(I)=LE(I-1)+BLOCK
          LE(I)=LB(I)+LANE
          If ((LB(I)+LANE) .gt. YR) LE(I)=YR
500           Continue
      Endif
 100  Return
      End
```

```
      SUBROUTINE Packinfo (M,N)
c**********************************************************************
c     This subroutine packs the values to be output into the arrays
c     that are passed in the common labeled Urban5. The data are indexed as follows:
c     Index1    = 1 for nonground reflected rays, 2 for ground reflected rays
c     Index2    = index of ray from 1 to 2*MAXR+1 for the rays with N from -MAXR to
c                 MAXR
c     Index3    = index of reflection point for each ray, from 1 to MAXR, with MAXR+1
c                 used for ground reflection point
c     PATHLENGTH(Index1,Index2)= double precision path length
c     ANGLE(Index1,Index2,1)=azimuth of ray at tx, pos=right,neg=left
c       "  (  "  ,  "  ,2)=elevation angle of ray at tx
c       "  (  "  ,  "  ,3)=azimuth of ray at rx, pos=right,neg=left
c       "  (  "  ,  "  ,4)=elevation angle of ray at rx
c       "  (  "  ,  "  ,5)=angle of reflection from normal to walls
c       "  (  "  ,  "  ,6)=  "   "   "      from normal to ground
c     REFLECTPTS(Index1,Index2,Index3,1)=X co-ordinate, reflection pt
c         "   (  "  ,  "  ,  "  ,2)=Y     "     ,     "     "
c         "   (  "  ,  "  ,  "  ,3)=Z     "     ,     "     "
c
c     Other variables:
c     M         = image index, 1= above ground, -1= below ground
c     N         = image index, 0= real location, neg=left, pos=right
c     MAXR      = maximum number of wall reflections a ray is allowed
c     TDIST     = true distance between TX and M,N RX image
c     AZMUTHTX  = azmuthal angle from TX to M,N RX image
c     ELEVATTX  = elevation angle from TX to M,N RX image
c     AZMUTHRX  = azmuthal angle from M,N RX image to TX
c     ELEVATRX  = elevation angle from M,N RX image to TX
c     GROUNDANG = angle of ground reflection with respect to grazing
c     WALLANG   = angle of wall reflection with respect to grazing
c   REFLECTIONS(INDEX1,INDEX2)= locations of reflection points for a particular ray
where:
c                INDEX1=1 to abs(N) is the wall reflection number
c                       =abs(N)+1 for the ground reflection
c                INDEX2=1 for X co-ordinate of reflection location
c                       =2  "  Y     "     "     "        "
c                       =3  "  Z     "     "     "        "
c**********************************************************************
```

```
      Common /Urban1/ MAXR,XT,YT,ZT,XR,YR,ZR,XI,YI,ZI,WIDTH
      Common /Urban2/ PATHDX,PATHDY,PATHDZ,HDIST,TDIST
      Common /Urban3/ AZMUTHTX,AZMUTHRX,ELEVATTX,ELEVATRX,
     +GROUNDANG,WALLANG
      Common /Urban4/ REFLECTIONS(11,3)
      Common /Urban5/ PATHLENGTH(2,21),ANGLE(2,21,6),
     +REFLECTPTS(2,21,11,3),OUT(2,21)
      Real*8 TDIST,HDIST,PATHLENGTH
c
c     Assign the index values for the ray
      INDEX1=Indexone (M)
      INDEX2=Indextwo (MAXR,N)
c
c     Pack the pathlength of the ray
      PATHLENGTH(INDEX1,INDEX2)=TDIST
c
c     Pack the angles for the ray
      ANGLE(INDEX1,INDEX2,1)=AZMUTHTX
      ANGLE(INDEX1,INDEX2,2)=ELEVATTX
      ANGLE(INDEX1,INDEX2,3)=AZMUTHRX
      ANGLE(INDEX1,INDEX2,4)=ELEVATRX
      If (N.eq.0) Then
c     No wall reflection, set angle to 0
          ANGLE(INDEX1,INDEX2,5)=0
      Else
c     There is at least one wall reflection
          ANGLE(INDEX1,INDEX2,5)=WALLANG
      Endif
      If (M.eq.1) Then
c     No ground reflection, set angle to 0
          ANGLE(INDEX1,INDEX2,6)=0
      Else
c     There is a ground reflection
          ANGLE(INDEX1,INDEX2,6)=GROUNDANG
      Endif
```

```
c
c     Pack the locations of the reflection points of the ray
      If (N.eq.0) Then
c          No wall reflections
      Else
c          There are abs(N) wall reflections, so pack
           Do 100 I=1,abs(N)
           Do 200 J=1,3
           REFLECTPTS(INDEX1,INDEX2,I,J)=REFLECTIONS(I,J)
200         Continue
100        Continue
      Endif
      If (M.eq.1) Then
c          No ground reflection
      Else
c          There is a ground reflection, so pack
           I=abs(N)+1
           Do 300 J=1,3
           REFLECTPTS(INDEX1,INDEX2,I,J)=REFLECTIONS(I,J)
300        Continue
      Endif
      Return
      End
```

```
      SUBROUTINE Unpack (M,N)
c**********************************************************************
c     This subroutine unpacks the values
c     that are passed in the common labeled Urban5.
c     The data are indexed as follows:
c     Index1    = 1 for nonground reflected rays, 2 for ground eflected rays
c     Index2    = index of ray from 1 to 2*MAXR+1 for the rays with N from -MAXR to
c                 MAXR
c     Index3    = index of reflection point for each ray, from 1 to MAXR, with MAXR+1
c                 used for ground reflection point
c     PATHLENGTH(Index1,Index2)= double precision path length
c     ANGLE(Index1,Index2,1)=azimuth of ray at tx, pos=right,neg=left
c       " ( "  , "  ,2)=elevation angle of ray at tx
c       " ( "  , "  ,3)=azimuth of ray at rx, pos=right,neg=left
c       " ( "  , "  ,4)=elevation angle of ray at rx
c       " ( "  , "  ,5)=angle of reflection from normal to walls
c       " ( "  , "  ,6)= "  "  "     from normal to ground
c     REFLECTPTS(Index1,Index2,Index3,1)=X co-ordinate, reflection pt
c         "  ( "  , "  , "  ,2)=Y    "   ,    "   "
c         "  ( "  , "  , "  ,3)=Z    "   ,    "   "
c
c     Other variables:
c     M           = image index, 1= above ground, -1= below ground
c     N           = image index, 0= real location, neg=left, pos=right
c     MAXR        = maximum number of wall reflections a ray is allowed
c     TDIST       = true distance between TX and M,N RX image
c     AZMUTHTX    = azmuthal angle from TX to M,N RX image
c     ELEVATTX    = elevation angle from TX to M,N RX image
c     AZMUTHRX    = azmuthal angle from M,N RX image to TX
c     ELEVATRX    = elevation angle from M,N RX image to TX
c     GROUNDANG   = angle of ground reflection with respect to grazing
c     WALLANG     = angle of wall reflection with respect to grazing
c     REFLECTIONS(INDEX1,INDEX2)= locations of reflection points for
c               a particular ray where:
c               INDEX1=1 to abs(N) is the wall reflection number
c                      =abs(N)+1 for the ground reflection
c               INDEX2=1 for X co-ordinate of reflection location
c                      =2 " Y    "    "    "      "
c                      =3 " Z    "    "    "      "
c**********************************************************************
```

```
      Common /Urban1/ MAXR,XT,YT,ZT,XR,YR,ZR,XI,YI,ZI,WIDTH
      Common /Urban2/ PATHDX,PATHDY,PATHDZ,HDIST,TDIST
      Common /Urban3/ AZMUTHTX,AZMUTHRX,ELEVATTX,ELEVATRX,
     +GROUNDANG,WALLANG
      Common /Urban4/ REFLECTIONS(11,3)
      Common /Urban5/ PATHLENGTH(2,21),ANGLE(2,21,6),
     +REFLECTPTS(2,21,11,3),OUT(2,21)
      Real*8 TDIST,HDIST,PATHLENGTH
c
c     Assign the index values for the ray
      INDEX1=Indexone (M)
      INDEX2=Indextwo (MAXR,N)
c
c     Unpack the pathlength of the ray
      TDIST=PATHLENGTH(INDEX1,INDEX2)
c
c     Unpack the angles for the ray
      AZMUTHTX=ANGLE(INDEX1,INDEX2,1)
      ELEVATTX=ANGLE(INDEX1,INDEX2,2)
      AZMUTHRX=ANGLE(INDEX1,INDEX2,3)
      ELEVATRX=ANGLE(INDEX1,INDEX2,4)
      If (N.eq.0) Then
c     No wall reflection, set angle to 0
          WALLANG=0
      Else
c     There is at least one wall reflection
          WALLANG=ANGLE(INDEX1,INDEX2,5)
      Endif
      If (M.eq.1) Then
c     No ground reflection, set angle to 0
          GROUNDANG=0
      Else
c     There is a ground reflection
          GROUNDANG=ANGLE(INDEX1,INDEX2,6)
      Endif
```

```
c
c     Unpack the locations of the reflection points of the ray
      If (N.eq.0) Then
c         No wall reflections
      Else
c         There are abs(N) wall reflections, so unpack
          Do 100 I=1,abs(N)
          Do 200 J=1,3
          REFLECTIONS(I,J)=REFLECTPTS(INDEX1,INDEX2,I,J)
200       Continue
100       Continue
      Endif
      If (M.eq.1) Then
c         No ground reflection
      Else
c         There is a ground reflection, so unpack
          I=abs(N)+1
          Do 300 J=1,3
          REFLECTIONS(I,J)=REFLECTPTS(INDEX1,INDEX2,I,J)
300       Continue
      Endif
      Return
      End
```

```
      FUNCTION trueangl(A1,B1,C1,A2,B2,C2)
c**********************************************************************
c     This subfunction returns the true angle between two lines in
c     three dimensional space.  The lines are assumed to intersect
c     one another. The formula is from GEOMETRY OF SPATIAL FORMS,
c     P.C. Gasson, 1983.  The a,b,c's are the direction ratios, i.e.,
c     the slopes except for a common multiplicative constant.
c**********************************************************************
      Real*8 A,B,C,D,E,F,NUMERATOR,DENOMINATOR,COSANG
      A=A1
      B=B1
      C=C1
      D=A2
      E=B2
      F=C2
      NUMERATOR=A*D+B*E+C*F
      DENOMINATOR=DSQRT(A*A+B*B+C*C)*DSQRT(D*D+E*E+F*F)
      COSANG=NUMERATOR/DENOMINATOR
      TRUEANGL=dacos(COSANG)
      Return
      End


c---------------------------------------------------------------
      FUNCTION Raddeg (Angrad)
c**********************************************************************
c     This function converts from radians to degrees.
c**********************************************************************
      Raddeg=57.2958*Angrad
      Return
      End


c---------------------------------------------------------------
      FUNCTION Degrad (Angdeg)
c**********************************************************************
c     This function converts from degrees to radians.
c**********************************************************************
      Degrad=Angdeg/57.2958
      Return
      End
```

```
c-----------------------------------------------------------------
      FUNCTION Indexone (M)
c***********************************************************************
c     This function sets the value of INDEX1 for the pack routines.
c***********************************************************************
c     write (1,*) m
      If (M .eq. 1) Then
c           This is an above ground image, no ground reflection
            Indexone=1
      Else
c           This is a below ground image, there is a ground reflection
            Indexone=2
      Endif
      Return
      End


c-----------------------------------------------------------------
      FUNCTION Indextwo (MAXR,N)
c***********************************************************************
C     This function sets the value of INDEX2 for pack routines.
c***********************************************************************
c     write (1,*) maxr,n
      Indextwo=MAXR+N+1
      Return
      End
```

FORM **NTIA-29**
(4-80)

U.S. DEPARTMENT OF COMMERCE
NAT'L. TELECOMMUNICATIONS AND INFORMATION ADMINISTRATION

BIBLIOGRAPHIC DATA SHEET

	1. PUBLICATION NO.	2. Gov't Accession No.	3. Recipient's Accession No.

4. TITLE AND SUBTITLE

A MODEL OF MILLIMETER-WAVE PROPAGATION FOR PERSONAL COMMUNICATION NETWORKS IN URBAN SETTINGS

5. Publication Date

6. Performing Organization Code
NTIA/ITS

7. AUTHOR(S)
K.C. ALLEN

9. Project/Task/Work Unit No.
910 1108

8. PERFORMING ORGANIZATION NAME AND ADDRESS
National Telecommunications and Information Admin.
Institute for Telecommunication Sciences
325 Broadway
Boulder, CO 80303

10. Contract/Grant No.

11. Sponsoring Organization Name and Address

NTIA

12. Type of Report and Period Covered

13.

14. SUPPLEMENTARY NOTES

15. ABSTRACT *(A 200-word or less factual summary of most significant information. If document includes a significant bibliography or literature survey, mention it here.)*

Rapid development of personal, portable, radio communications is expected during this decade. A primary example of this is the emergence of personal communication networks (PCN). These networks are similar to today's cellular telephone technology. However, much smaller cell sizes are used and, as a result, the portable phone is much smaller (pocket size) and inexpensive. The use of millimeter waves for PCN services offers many advantages. Models of millimeter-wave propagation on the kinds of paths that will occur in small cells are needed. In this report a geometrical optics model of the propagation of millimeter waves for line-of-sight paths near street level in urban environments is developed. An idealized environment is assumed with flat streets and uniform street widths between flat building walls. The image-space approach is used to index the direct line-of-sight ray and all reflected ray paths between the transmitter and receiver. The model can be used to simulate received signal characteristics for testing system designs. The statistical behavior of signal characteristics for testing (continuted)

16. Key Words *(Alphabetical order, separated by semicolons)*
impulse response; millimeter waves; PCN; personal communication networks; propagation; urban

17. AVAILABILITY STATEMENT

☒ UNLIMITED.

☐ FOR OFFICIAL DISTRIBUTION.

18. Security Class. *(This report)*
Unclassified

20. Number of pages
88

19. Security Class. *(This page)*
Unclassified

21. Price:

15. Abstract (Continued)

system designs. The statistical behavior of signal level can be computed from the model for real world environments for which it is not practical to give a complete description of the complex physical geometry. The model also shows the channel impulse response functions to be expected in urban cells. Calculations from the model are compared with data measured in downtown Denver at 9.6, 28.8, and 57.6 GHz.

☆ U.S. GOVERNMENT PRINTING OFFICE: 1991–573-002/21,058